LUND UNIVERSITY

Structure, oxidation, and catalytic activity of platinum-tin surfaces

Wallander, Harald

2024

Link to publication

Citation for published version (APA):
Wallander, H. (2024). *Structure, oxidation, and catalytic activity of platinum-tin surfaces*. [Doctoral Thesis (compilation), Lund University]. Lunds universitet.

Total number of authors:
1

General rights
Unless other specific re-use rights are stated the following general rights apply:
Copyright and moral rights for the publications made accessible in the public portal are retained by the authors and/or other copyright owners and it is a condition of accessing publications that users recognise and abide by the legal requirements associated with these rights.
- Users may download and print one copy of any publication from the public portal for the purpose of private study or research.
- You may not further distribute the material or use it for any profit-making activity or commercial gain
- You may freely distribute the URL identifying the publication in the public portal

Read more about Creative commons licenses: https://creativecommons.org/licenses/

Take down policy
If you believe that this document breaches copyright please contact us providing details, and we will remove access to the work immediately and investigate your claim.

LUND UNIVERSITY

PO Box 117
221 00 Lund
+46 46-222 00 00

Structure, oxidation, and catalytic activity of platinum-tin surfaces

HARALD WALLANDER
DEPARTMENT OF PHYSICS | FACULTY OF SCIENCE | LUND UNIVERSITY

Printed by Media-Tryck, Lund 2024 NORDIC SWAN ECOLABEL 3041 0903

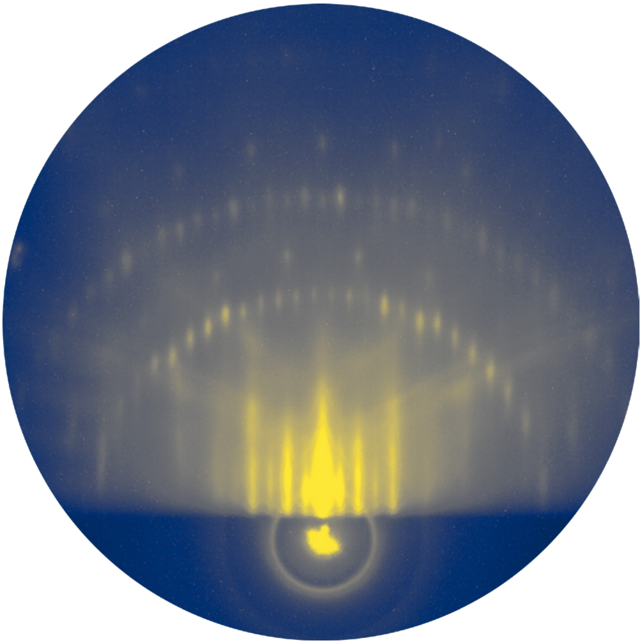

Faculty of Science
Department of Physics
Synchrotron Radiation Research

ISBN 978-91-8104-155-2

Structure, oxidation, and catalytic activity of platinum-tin surfaces

Structure, oxidation, and catalytic activity of platinum-tin surfaces

by Harald Wallander

LUND
UNIVERSITY

Thesis for the degree of Doctor of Philosophy
Thesis advisors: Docent Lindsay R. Merte, Prof. Edvin Lundgren, Docent Johan Gustafson
Faculty opponent: Dr. David E. Starr

To be presented, with the permission of the Faculty of Science of Lund University, for public criticism in the Rydberg lecture hall (Rydbergsalen) at the Department of Synchrotron radiation research on Friday, the 4th of October 2024 at 13:15.

DOKUMENTDATABLAD enl SIS 61 41 21

Organization
LUND UNIVERSITY

Department of Synchrotron radiation research
Box 118
SE–221 00 LUND
Sweden

Document name
DOCTORAL DISSERTATION

Date of disputation
2024-10-04

Sponsoring organization

Author(s)
Harald Wallander

Title and subtitle
Structure, oxidation, and catalytic activity of platinum-tin surfaces

Abstract

This thesis work has focused on the platinum-tin surface, especially how it behaves when exposed to gases like oxygen and carbon monoxide. Platinum-tin is used as a catalyst for a range of reactions, including the oxidation of carbon monoxide at mild conditions, which is important for gas purification in fuel cells. The platinum-tin alloy has properties useful for the reactions it catalyses, but it is known that the tin in the catalyst oxidises during reaction conditions. What is not known is what roles these oxides play in the reactions.

Our efforts have been spent on trying to understand the oxide phases that form on the platinum-tin surface and how they behave under CO oxidation conditions. We have studied two related surface oxides with (4×4) and $(2m \times 2n)$ periodicities in ultra high vacuum conditions. They form during the initial stages of oxidation on the $Pt_3Sn(111)$ surface with the $(2m \times 2n)$ oxide having a higher oxygen content than the (4×4) oxide. The growth and transformations of these oxides was studied using scanning tunnelling microscopy, low energy electron microscopy and low energy electron diffraction, surface x-ray diffraction and density functional theory. Transformations between these oxides are driven by exposure to oxygen or carbon monoxide, indicating that they may have a role in the CO oxidation reaction.

We have also studied platinum-tin surfaces operando during CO oxidation at millibar pressures. The tin in the platinum-tin surface oxidises under reaction conditions and this lowers the activity of the surface. The oxidised platinum-tin surfaces are more active for CO oxidation than the platinum surfaces studied, and the activity is linked to platinum-tin alloy or Sn(II) surface oxides. The gas composition and pressure affects the composition and morphology of the oxide that forms, and at sufficient temperatures CO can reduce the tin oxides. This reduction requires exposed oxide edge sites. The reduction of the tin oxides does not appear to be a main contributor to the CO oxidation activity.

Key words
Surface Science, Catalysis, Platinum, Tin, CO oxidation, X-ray Photoelectron Spectroscopy, X-ray Absorption Spectroscopy, Surface X-ray Diffraction, Scanning Tunnelling Microscopy, Density Functional Theory

Classification system and/or index terms (if any)

Supplementary bibliographical information

Language
English

ISSN and key title

ISBN
978-91-8104-155-2 (print)
978-91-8104-156-9 (pdf)

Recipient's notes

Number of pages
179

Price

Security classification

I, the undersigned, being the copyright owner of the abstract of the above-mentioned dissertation, hereby grant to all reference sources the permission to publish and disseminate the abstract of the above-mentioned dissertation.

Signature ________________________ Date 2024-08-19

Structure, oxidation, and catalytic activity of platinum-tin surfaces

by Harald Wallander

Lund
University

A doctoral thesis at a university in Sweden takes either the form of a single, cohesive research study (monograph) or a summary of research papers (compilation thesis), which the doctoral student has written alone or together with one or several other author(s).

In the latter case the thesis consists of two parts. An introductory text puts the research work into context and summarizes the main points of the papers. Then, the research publications themselves are reproduced, together with a description of the individual contributions of the authors. The research papers may either have been already published or are manuscripts at various stages (in press, submitted, or in draft).

Cover illustration front: A Scanning Tunnelling Microscopy (STM) image of a tin surface oxide island on top of a $Pt_3Sn(111)$ surface. This surface oxide is the so-called ”stripe phase” described in paper V. Image recorded by Lindsay Merte.

Cover illustration back: A Reflection High Energy Electron Diffraction (RHEED) image of tin surface oxide on top of a Pt(111) surface. The surface oxide has a (4×4) periodicity, visible in the image.

Funding information: The thesis work was financially supported by Vetenskapsrådet and Knut and Alice Wallenberg Foundation.

© Harald Wallander 2024

Faculty of Science, Department of Synchrotron radiation research

ISBN: 978-91-8104-155-2 (print)
ISBN: 978-91-8104-156-9 (pdf)

Printed in Sweden by Media-Tryck, Lund University, Lund 2024

Printed matter
3041 0903

Media-Tryck is a Nordic Swan Ecolabel
certified provider of printed material.
Read more about our environmental
work at www.mediatryck.lu.se

MADE IN SWEDEN

To my family and friends

Contents

Preface v

List of publications v

List of abbreviations viii

Popular summary in English ix

Populärvetenskaplig sammanfattning på svenska xi

Acknowledgements xiii

Structure, oxidation, and catalytic activity of platinum-tin surfaces 3

1 Introduction 3

2 Catalysis 7

1 Fundamental concepts 8

2 Real systems and model systems 10

3 CO oxidation 11

3 Crystals and crystal surfaces 13

1 Crystals 14

2 Surfaces 15

3 Thin films and 2D materials 16

4 Platinum-tin 17

Platinum 17

Tin and its oxides 18

4.1 Properties of platinum-tin 19

4.2 Platinum-tin surfaces 19

4.3 CO oxidation over Platinum-tin 23

4 Methods 25

0.1 Electrons and x-rays as probes 26

0.2 Synchrotrons 27

0.3 The photoelectric effect 28

1 Spectroscopy 31

1.1 X-ray Photoelectron Spectroscopy (XPS) 31

Experimental setup for XPS 36

Near Ambient Pressure XPS (NAP-XPS) 37
1.2 X-ray Absorption Spectroscopy (XAS) 38
Experimental setup for XAS 42
1.3 Auger Electron Spectroscopy (AES) 43
2 Diffraction 44
2.1 Surface X-Ray Diffraction (SXRD) 45
2.2 Reflection High Energy Electron Diffraction (RHEED) 46
2.3 Low Energy Electron Diffraction (LEED) 47
3 Microscopy 48
3.1 Low Energy Electron Microssopy (LEEM) & Photo Emission Electron Microscopy (PEEM) 48
3.2 Scanning Tunnelling Microscopy (STM) & Atomic Force Microscopy (AFM) 50
4 Computational techniques 52
4.1 Density Functional Theory (DFT) 52
4.2 Machine learning 52
5 Mass spectrometry (MS) 53

5 Summary of the research papers 55

6 Outlook 59

7 References 61

Scientific publications 75
Paper I: Oxidation of a Platinum–Tin Alloy Surface during Catalytic CO Oxidation 75
Paper II: Dynamic Behavior of Tin at Platinum Surfaces during Catalytic CO Oxidation 87
Paper III: Platinum-Tin surface alloys studied during O_2 exposure, and CO oxidation using grazing-incidence XANES 99
Paper IV: Cleaning and tailoring the $Pt_3Sn(111)$ surface for surface experiments 115
Paper V: Oxygen Storage by Tin Oxide Monolayers on $Pt_3Sn(111)$ 127
Paper VI: Growth, structure, and morphology of ultra-thin tin oxide phases forming on $Pt_3Sn(111)$ upon exposure to oxygen 137

Preface

List of publications

This thesis is based on the following publications, referred to by their Roman numerals:

I **Oxidation of a Platinum–Tin Alloy Surface during Catalytic CO Oxidation**

H. J. Wallander, Freddy E. Oropeza,- Benjamin Hagman, Jan Knudsen, Edvin Lundgren, and Lindsay R. Merte
J. Phys. Chem. C 2022, 126, 14, pp. 6258–6266

I participated in the collection of part of the experimental data at MAX IV, performed the data analysis, and prepared the first draft of the manuscript. I coordinated the preparation of the final version of the manuscript based on input from the co-authors and reviewers.

II **Dynamic Behavior of Tin at Platinum Surfaces during Catalytic CO Oxidation**

H. J. Wallander, Dorotea Gajdek, Stefano Albertin, Gary Harlow, Nicolas Braud, Lars Buß, Jon-Olaf Krisponeit, Jan Ingo Flege, Jens Falta, Edvin Lundgren, and Lindsay R. Merte
ACS Catal. 2023, 13, 24, pp. 16158–16167

I was the main responsible for organizing and running the experiment at MAX IV, performed the data analysis, and prepared the first draft of the manuscript. I coordinated the preparation of the final version of the manuscript based on input from the co-authors and reviewers.

III **Platinum-Tin surface alloys studied during O_2 exposure, and CO oxidation using grazing-incidence XANES**
H. J. Wallander, Dorotea Gajdek, Gary Harlow, Jakob Blomqvist, Justus Just, Matteo Ciambezi, Edvin Lundgren, and Lindsay R. Merte
Submitted manuscript

I was the main responsible for organizing and running the experiment at MAX IV, performed the data analysis, and prepared the first draft of the manuscript. I coordinated the preparation of the final version of the manuscript based on input from the co-authors and reviewers.

IV **Cleaning and tailoring the $Pt_3Sn(111)$ surface for surface experiments**

N. Braud, L. Buß, E. Lundgren, L.R. Merte, H. Wallander, J.-O. Krisponeit, A. Locatelli, T.O. Mentes, M. Jugovac, J.I. Flege, J. Falta
Surface Science, Volume 732, 2023, 122281, ISSN 0039-6028,

I contributed to the design of the experiments, the interpretation of the data, and the review and editing of the final manuscript.

V **Oxygen Storage by Tin Oxide Monolayers on $Pt_3Sn(111)$**

L. R. Merte, Nicolas Braud, Lars Buß, Malthe Kjær Bisbo, Harald J. Wallander, Jon-Olaf Krisponeit, Jan Ingo Flege, Bjørk Hammer, Jens Falta, and Edvin Lundgren
J. Phys. Chem. C 2023, 127, 6, pp. 2988–2994

I contributed to the interpretation of the data, and to the review and editing of the final manuscript.

VI **Growth, structure, and morphology of ultra-thin tin oxide phases forming on $Pt_3Sn(111)$ upon exposure to oxygen**
N. Braud, H. J. Wallander, L. Buß, L.R. Merte, J. Blomqvist, M. Löfstrand, E. Lundgren, T. Schmidt, J-O. Krisponeit, J.I. Flege, J. Falta
Manuscript in preparation

I was the main responsible for organizing and running the surface x-ray diffraction experiment at SOLEIL, and the x-ray photo electron spectroscopy experiment at Flex PES at MAX IV. I performed the analysis of these data and provided the figures and text related to these data. I contributed to the interpretation of the data and to the review and editing of the final manuscript.

Publications that I have co-authored but are not included in this thesis:

Simulated sample heating from a nanofocused X-ray beam

H. J. Wallander, J. Wallentin
J. Synchrotron Rad. 24, 925–933 (2017)

Stroboscopic operando spectroscopy of the dynamics in heterogeneous catalysis by event-averaging.
J. Knudsen, T. Gallo1, V. Boix, M. Døvre Strømsheim, G. D'Acunto, C. Goodwin, H. J. Wallander, S. Zhu, M. Soldemo, P. Lömker, F. Cavalca, M. Scardamaglia, D. Degerman, Anders Nilsson, P. Amann, A. Shavorskiy, J. Schnadt
Nat Commun 12, 6117 (2021)

In Situ H_2 Reduction of Al_2O_3-Supported Ni- and Mo-Based Catalysts

S. M. Gericke, J. Rissler, M. Bermeo, H. J. Wallander, H. Karlsson, L. Kollberg, M. Scardamaglia, R. Temperton, S. Zhu, K. G. V. Sigfridsson Clauss, C. Hulteberg, A. Shavorskiy, L. R. Merte, M. E. Messing, J. Zetterberg, S. Blomberg
Catalysts 2022, 12(7), 755

Operando XANES Reveals the Chemical State of Iron-Oxide Monolayer During Low-Temperature CO Oxidation
D. Gajdek, H. J. Wallander, G. Abbondanza, G. Harlow, J. Gustafson, S. Blomberg, P.-A. Carlsson, J. Just, E. Lundgren, and L.y R. Merte
Manuscript in preparation

Structure of few-layer cobalt oxides on Pt(111)

D. Gajdek*, **H. J. Wallander***, E. Lundgren, L. R. Merte
Manuscript in preparation

List of abbreviations

AES	Auger Emission Spectroscopy
AFM	Atomic Force microscopy
BCC	Body Centered Cubic
BCT	Body Centered Tetragonal
CCD	Charge Coupled Device
CL	Core Level
CLS	Core Level Shift
DFT	Density Functional Theory
ESCA	Electron Spectroscopy for Chemical Analysis
EXAFS	Extended X-ray Absorption Fine Structure
FCC	Face Centered Cubic
FWHM	Full Width Half Maximum
HCP	Hexagonal Cole Packed
LEED	Low Energy Electron Diffraction
LEEM	Low Energy Electron Microscopy
LCA	Linear Combination Analysis
MCP	Multi Channel Plate
ML	Mono Layer
MS	Mass Spectrometry
NP	Nano Particle
(X-)PEEM	(X-ray) Photo Electron Emission Microscopy
RHEED	Reflection High Energy Electron Diffraction
SC	Simple Cubic
SEM	Scanning Electron Microscopy
SMSI	Strong Metal Support Interaction
ST	Simple Tetragonal
STM	Scanning Tunnelling Microscopy
TEM	Transmission Electron Microscopy
TPD	Temperature Programmed Desorption
UHV	Ultra High Vacuum
UV	Ultra Violet
XAFS	X-ray Absorption Fine Structure
XAS	X-ray Absorption Spectroscopy
XANES	X-ray Absorption Near Edge Structure
(NAP-)XPS	(Near Ambient Pressure) X-ray Photo emission Spectroscopy
(S-)XRD	(Surface) X-Ray Diffraction

Popular summary in English

If you had a tool you relied on, you would probably want to know how it works. Or at least that someone knows, even if you don't have a detailed understanding on how your laptop or telephone works you can rest assured that someone does know and can fix it or develop a better version for the future. But what if *no one* really knew? This is the case (to some extent) with catalysts, the materials that are used to produce almost every chemical product we use. This includes fuels, consumer goods, and fertilisers. Most catalysts have been found by trial-and-error, for some of them no one really knows why they work. Catalysts rely on how molecules interact with each other on its surface. The molecules have their exits and their entrances; and one molecule in its time plays many parts. Much like us. But this play is invisible to us, and it is played out thousands of times faster than we can follow. Still, there are ways we can learn about what goes down between the molecules down there on their nano-scaled stage.

One catalyst that we don't know how it works is platinum-tin. It is used for many things, one example is in fuel cells. Fuel cells are devices that can transform chemical fuels such as hydrogen or alcohols directly into electricity, and they are attracting a fair amount of interest now that the electrification of society is taking off. They rely completely on catalysts such as platinum-tin to operate, but we don't know exactly how it works. If we did, we could perhaps improve it so that it worked several times better, or maybe we could even replace the very expensive platinum that is often in them with something cheaper. We want to know how it works.

The tin in platinum-tin is in a dilemma. Tin is not noble, and it has a hard time resisting reacting with oxygen. At the same time, it really likes being mixed up with the noble platinum. What to do? As a result, tin often tries to hang with both and end up in strange configurations between oxygen and platinum. Some of these configurations, surface oxides as we would call them, have rather interesting qualities compared to normal oxides. Platinum-tin is used to oxidise carbon monoxide to carbon dioxide (a crucial reaction in a fuel cell). Together, platinum and tin can do the job that platinum usually does, but with less effort. The cheap tin makes the expensive platinum better. But was the tin mixed with the platinum, in the oxide, or something in between when the reaction took place? Do the surface oxides have anything to do with the reaction? We have investigated.

Using x-rays and electrons, we have seen what the tin and platinum do when oxygen and carbon monoxide are around. With spectroscopy, we can see how many oxygen the tin has around it at any time. When the gas molecules arrive and the temperature gets higher, tin goes with the oxygen to form an oxide. If the tin goes completely with the oxygen (to tin dioxide, the most stable tin oxide), there is no longer any improved activity for the reaction. If the tin goes into one of these in-between surface oxides, some of the activity improvement is kept. Sometimes the surface oxides even seem to be able to do the job even without the direct involvement of platinum. If carbon monoxide can get down to the platinum and it is hot enough, it makes short work of the tin-oxygen friendship: it removes the oxygen from the tin oxide, which goes back to metallic form. The carbon monoxide really needs the platinum for that though, it cant go it alone directly from the gas. These experiments showed us how much the gas composition and the state of the platinum-tin surface affect each other. It also showed how the in-between surface oxides behave in gas.

Using diffraction and microscopy we saw how the surface oxides looked like in detail, in more controlled conditions. Only a few gas molecules were around here and there, but in exchange we could see more. There are two kinds of in-between surface oxides: In one of them the tin has a few more oxygen atoms around it, but they leave when carbon monoxide comes around. This could be a way in which the tin in platinum-tin helps running the reaction from carbon monoxide to carbon dioxide.

So we have gained a deeper understanding of the surface oxides the tin forms when it is around platinum and oxygen, and we have seen how the gas and the oxides affect each other. The surface oxides can make previously well-known materials (like tin oxides) behave in new ways. If we had a better understanding of them, maybe we could develop efficient catalysts from cheaper materials than platinum, or make new materials with novel properties. We have taken a few steps along the way, but there is much more to discover.

Populärvetenskaplig sammanfattning på svenska

Om du hade ett verktyg du verkligen var beroende av, hade du nog velat veta hur det fungerade. Eller åtminstone vara säker på att någon viste: även om du inte förstår precis hur din dator eller telefon fungerar finns det någon som kan fixa eller förbättra den. Men om *ingen* viste? Så är det (till viss del) med katalysatorer, materialen vi använder för att producera nästan alla kemikalier vi använder. Det gäller allt från bränslen, konsumtionsvaror, till konstgödsel. Men ingen vet -precis- hur de fungerar: de flesta katalysatorer har upptäckts genom att man försökt få fram något som funkade på måfå. Vi vet i alla fall att katalysatorer binder molekyler till sin yta, där de sedan kan reagera med varandra. Molekylerna spelar olika roller på katalysatorns yta och har sina entréer och sortier, likt skådespelare på en scen. Men pjäsen är osynlig för oss, och utspelar sig tusentals gånger snabbare än vad vi kan uppfatta. Det finns dock sätt för oss att lära oss något om vad som händer molekylerna emellan, där nere på deras nanoscen.

En katalysator vi inte vet hur den funkar är platina-tenn. Den används till mycket, ett exempel är i bränsleceller. Bränsleceller är apparater som kan omvandla bränsle som vätgas eller alkohol direkt till elektricitet, och de börjar bli mer och mer intressanta nu när elektrifieringen av samhället börjar ta fart. De är helt beroende av katalysatorer för att fungera, men vi vet ju inte riktigt hur de fungerar. Gjorde vi det hade vi kanske kunnat förbättra dem så att de blev flera gånger bättre, eller till och med ersätta den väldigt dyra platinan de ofta inehåller med något billigare. Vi vill veta hur de fungerar.

Tennet i platina-tennlegeringen dras mellan två starka krafter. Tenn är inte ädelt, så det reagerar gärna med syre (det oxiderar). Samtidigt gillar det att vara med den ädla platinan. Vad ska det göra? Tennet försöker ofta vara med båda, vilket leder till att det hamnar i märkliga positioner emellan platina och syre. Tennet är då delvis oxiderat, men också bundet till platinaytan. Vi kallar det som bildas för en ytoxid, och de har nya egenskaper vanliga oxider inte har. Vissa av dessa ytoxider har ganska intressanta egenskaper när det kommer till hur de interagerar kemiskt med andra ämnen. Platina-tenn används till att oxidera kolmonoxid till koldioxid (vilket är nödvändigt för att t.ex. en bränslecell ska fungera). Tillsammans oxiderar platina-tenn kolmonoxiden vid lägre temperatur än vad platinan gör ensamt, det billiga tennet gör alltså den dyra platinan bättre. Men hur? Är tennet blandat med platinan, oxiderat, eller något mitt emellan när reaktionen sker? Hur påverkar de speciella ytoxiderna reaktionen? Det har vi undersökt.

Med hjälp av röntgenstrålning och elektronstrålning har vi sett vad tennet gör när syre och kolmonoxid är närvarande. Med spektroskopi kan vi se hur många syreatomer tennet har omkring sig vid varje tillfälle. När gasmolekylerna anländer och temperaturen stiger reagerar tennet med syret och bildar en oxid. Vilken slags oxid beror på hur sammansättningen på gasen ser ut. Om tennet reagerar helt med syret (till tenndioxid, den mest stabila formen) blir det ingen förbättring av aktiviteten för oxideringen av kolmonoxid: platinan gör nu hela jobbet. Om tennet i stället blir en av de där mitt-emellan ytoxiderna är dock en del av den förbättrade aktiviteten bevarad. Ibland ser det till och med ut som att ytoxiden kan göra jobbet själv, eller med endast indirekt hjälp av platinan. Om kolmonoxiden kan ta sig ned till platinan blir dock tennets vänskap med syret kort: kolmonoxiden reagerar med syret i oxiden, tennoxiden reduceras till metall och går tillbaka till platinan. Kolmonoxiden behöver dock platinan för denna reduktion, den pallar inte göra det själv direkt från gasen. Dessa experiment lärde oss hur mycket gasblandningen påverkar vad som händer på ytan och vice versa. De visade oss också hur de här ytoxiderna beter sig när de utsätts för gas.

Med mikroskopi och diffraktion kunde vi se hur ytoxiderna betedde sig under mer ordnade former. Bara några få gasmolekyler var med då och då, men å andra sidan kunde vi se desto mer. Det finns två former av den tunna ytoxiden vi studerat: i en av dem finns det mer syre än i den andra. Det extra syret försvinner fort när kolmonoxiden anländer. Denna ssyrelagringsmekansimskulle kunna vara ett sätt tennet i platina-tenn hjälper till att oxidera kolmonoxid till koldioxid.

Så för att summera så har vi fått en djupare förståelse av de där mitt-emellan ytoxiderna som tennet bildar på platina-tennytan, vi har sett hur de beter sig när de utsätts för gas och hur detta påverkar reaktionen. Ytoxiderna gör det möjligt att få tidigare välkända material (som tennoxid) att bete sig på nya sätt. Kanske kan en bättre förståelse av dem göra det möjligt att utveckla katalysatorer av billigare material än platina, eller nya material med oanade egenskaper. Vi har tagit några steg på vägen, men det finns mycket kvar att utforska.

Acknowledgements

It is said that it takes a village to raise a child, and the same is true for doctors. My growth as a scientist, and as a person, has been shaped by the people that I have had around me during these five years. Some have been directly involved in my development, some I have worked together with, and some have been part of the community that I am now myself a part of. I have been fortunate enough to be surrounded by good people to learn from, get inspired by, and enjoy good times with.

First of all, I acknowledge the work and effort from my main supervisor **Lindsay Merte**. Your knowledge and insight is matched by few, and your readiness to share your knowledge has been a great asset during my PhD. You always make time to support your students, despite the constant shortage of time we are faced with, and take us seriously. I am pleased with the results of the work we produced, and part of the reason is that we both want to make things right and not cut corners. I have appreciated that attitude.

My second supervisor **Edvin Lundgren** has also been heavily involved in my PhD Work. Your great experience and perspective has been an important help in the work we have done together. Your friendliness, and sense of humour has also done a lot for the department to become such pleasant place to be in. Not to mention the collaborations it has sparked. My co-supervisor **Johan Gustafsson** has also helped me with scientific discussion and perspective coming from a different experimental technique.

One of the people I have been working most closely with is my fellow PhD student **Dorotea ”Dora” Gajdek**, which has been a pleasure. Your organisational skills have helped the team a lot, and on a more personal level your straight-forward, friendly attitude has made any group you have been part of nicer.

At the Synchrotron division at Lund University, good people are abundant. I want to mention my supervisor from my master thesis, **Jan Knudsen**. What I learned from you during my master thesis ended up being a big part of my PhD, and led to some fruitful collaboration. Thank you for setting me on the right path. **Jesper Wallentin**, who was my supervisor for my bachelor project, introduced me to synchrotrons. **Estephania Lira** is the laboratory technician and has helped me in my work with their STM. Many experiments and articles were produced together with **Gary Harlow** (now in the US). Thank you for helping us, and for your discerning eye making sure the science is up to scratch. I have spent some good times with current and former PhD students at the division too. **Alfred Larsson** and **Andrea Grespi**, thank you for the barbecues, activities and conversations. **Virgínia Boix**, **Tamires Gallo**, and **Stefano Albertin**, you were influential fellow students in my early days at the division. There are many more PhD students (and seniors) at the division I have spent time with as well, you are remembered although I do not list all your names!

From combustion physics **Lisa Rämish** and **Sabrina Gericke** have been two good companions during our parallel PhD journeys. **Sebastian Pfaff**, you also made an impact with your enthusiasm and humour. The team leader **Johan Zetterberg** also stepped in and helped me when I needed it, thank you for that. From chemical engineering I've worked with **Sara Blomberg**, it's always fun to be around your good attitude.

Some of the people I've spent the most time with during my PhD years are those from the Department of Materials Science and Applied Mathematics at Malmö University. **Samuele Sottile**, **Asimina Papoulia**, **Madeleine Burheim** (and Dora again), you were already in place as PhD students when I started. Thank you for giving me a small, but great group to join. Thank you Madeleine for also helping me as a new teacher, a new skill that I am glad I got to develop. **Grzegorz "Greg" Sadowski**, **Shilpa Bijavara Seshashayana**, **Mattias Tidefelt**, **Indrajeet Tambe**, **Sana Khayyamifar**, **Miguel Kofoed**, **Andrea Morales Rodríguez**, and **Pedro Moya**, you started after me. What a pleasure it has been to see our originally small group grow into a quite large group, and to see our office culture develop into the friendly, supporting, and fun-loving space that it is today. Some honourable mentions go out to Greg for arranging our board games sessions (and your dad jokes) and our master-of-memes Shilpa (among others). It was great fun taking the shipping licence together, Mattias, and discussing life. I also got the opportunity to supervise the master student **Mats Löfstrand**. Thank you for your help with beamtimes, your curiosity, and positive attitude. There are also seniors and administrators at the department, and they deserve mention. Thank you **Jakob Blomqvist** for helping us with beamtimes, thank you **Henrik Hartman** and **Pär Olsson** for helping me teaching in your courses, thank you **Katja Frid** and **Mats Persson** for making sure the department was running as it should, thank you **Christina Bjerkén** for caring for the environment and sustainability. Thank you **Solveig-Karin Erdal** for the tomato seeds, the resulting tomato plants are growing vigorously on my balcony at this very moment. Thank you **Andreas Krause** and **Milan Burke** for hanging out with us PhD students, you are great company. The PhD students at the Department of Computer Science and Media Technology are also good company. In the establishment of our very own lab, **Peter Falkman** has been very helpful.

I have had the fortune to collaborate a bit more closely with the research group led by **Jens Falta** in Bremen. Thank you Jens, **Jan-Ingo Flege**, **Jan-Olaf Krisponeit**, **Thomas Schmidt**, **Nicolas Braud**, and **Lars Buß** for combining our expertise and techniques in researching platinum-tin together. LEEM is a cool technique.

Much of our work has depended completely on synchrotron facilities, and the scientists working at them. At HIPPIE at MAX IV **Jan Knudsen**, **Andrey Shavorskiy**, **Suyun Zhu** and **Mattia Scardamaglia** have been helping us a lot. At FlexPES **Alexei Preobrajenski** and **Andrey Generalov** have been good support. At BALDER **Justus Just** and **Matteo Ciambezi** helped us with our experiments. **Hadeel Hussein** at Diamond Light Source has been a great help for several of our experiments. **Andrea Resta** helped us at SOLEIL.

Also people outside of work have made an impact on me during my PhD student years. I want to thank my old and close friends **Simon Rosborg** and **Anna Isberg**. Our boat building project was a beautiful way to tackle the pandemic and its restrictions. I also want to thank the Lindy Hop and swing dance scene in Malmö and Lund (and the world), the joyful and friendly community you provide can turn the worst of days around.

The final thank you goes to my family. **Håkan Wallander** and **Inger Valeur**, my parents, thank you for your unwavering support and sharing of you own life experiences, giving me perspective. Thank you **Edvin Wallander**, dearest brother, for being a good brother. It is great for us to share our experiences, and for me to follow you during your own PhD journey. Every year I understand more and more how fortunate I am to have such an understanding, wise, and considerate family.

Structure, oxidation, and catalytic activity of platinum-tin surfaces

Chapter 1

Introduction

Our civilization is very prosperous; the abundance of food, the quality and variety of material goods is unparalleled in history. This feat is made possible by technological advances, but when we look down to see what underpins these advances, not all is clear. One of the most influential technologies that has improved our lives is catalysis, a tool for efficiently producing chemicals that we need for maintaining our society, making the products we use, and even building our own bodies (the artificial synthesis of ammonia is argued to be the most important invention of the last century [104], and that is just one example). In the big picture much is known about catalysis, but as they are tools for making molecules, the processes that govern them operate on the atomic scale. Gaining an understanding of these fundamental atomic-scale processes is challenging, and there are many gaps in our knowledge. Most catalysts have been discovered by trial-and-error, which means that we often do not know how efficient the catalyst is compared to how efficient it could have been. Often only a small fraction of the catalyst surface is taking part in the catalytic reaction. For this reason a more fundamental understanding of how catalysts work, on the atomic scale, is strongly desired by the scientific community. The promise, if we manage to gain this understanding, would be to fully optimise catalysts, making the best use of the (often expensive) materials, replace expensive materials with cheaper ones, and perhaps designing new materials with abilities not yet imagined. This is one of the main motivations for the field of surface science, of which this thesis work is a part.

Surface science as a field is concerned with what happens on the surface of a material on an atomic level. The applications of surface science are many, from the corrosion of metals, to semiconductors, and also catalyst surfaces. Real catalysts often consist of metal particles of nano meter size dispersed in a porous oxide support material. This is a complicated system that is difficult to study in detail, so the surface science approach is to use well defined metal surfaces of the catalytic material and study them in controlled conditions. The metal samples are often single crystals with well defined surface terminations, designed to mimic certain facets of a nano particle. The interaction between the metal surface and and oxide support material can be studied by adding oxide on top of the metal surface, the so-called ”inverse catalyst” approach. In this way many insights have been gained into the working principles of catalytic surfaces. Examples include the difference in activity between different facets, the role of edge sites and defects on the metal or oxide surface etc. However, even a well defined single crystal surface can be a complicated system and certain compromises have to be made in order to study them experimentally.

Despite the success of the surface science approach in the past few decades, many questions remain unanswered. An isolated single crystal surface is a complicated environment, as already mentioned, but it is simpler than a nano particle facet in a real catalytic system. This discrepancy is called the materials gap: how do we know what happens on the single crystal surface is what is also happening on the nano particle? Many of the techniques used in surface science also require some degree of vacuum to function (often mbar pressures or much lower), introducing the so called pressure gap. How do we know that what happens at very low pressure is relevant to a catalyst that is operated at or above atmospheric pressure? These questions motivates the development of techniques that can be used at higher pressures, or the study of materials more similar to the real catalyst than the single crystal surface. Many experimental techniques have been developed to push the limits of what pressures the can operate at, opening new possibilities for the study of materials and closing the pressure gap. The gradual study of more and more complex surfaces, for example introducing step sites on single crystal surfaces, or the study of nano particles of well defined size are approaches to closing the materials gap. Many surfaces can also form complex structures unique to the surface itself, and knowing how molecules and atoms interact and react on such surfaces can be difficult to disentangle, even for model systems.

This thesis work has been focused on platinum-tin surfaces. Platinum-tin is used industrially today for dehydrogenation of hydrocarbons [50, 25], electro-oxidation of alcohols [67, 59, 30, 118, 117] and CO [42, 43, 106, 105], and oxidation of CO in streams of H_2 at low temperatures [98, 3, 77]. The low temperature oxidation of CO is an important process in hydrogen-based fuel cells, where CO needs to be removed from the hydrogen gas stream before it reaches the fuel cell. It is crucial that only the CO is oxidised and not the hydrogen, and for this reason low temperatures are required. Platinum-tin is an interesting material as it is an alloy of the noble metal platinum and the no-so-noble metal tin. Tin oxidises much more easily than platinum, and a long standing question has been whether the tin in platinum-tin is oxidised or metallic when it partakes in the catalytic reaction. The tin oxides that form on platinum-tin surfaces also have complicated structures not seen on pure tin oxides. It is fundamental interest to study how these unique oxides behave, if they are present during reaction conditions, and if they participate in the catalytic reactions the platinum-tin catalyst is used for.

In paper I, we exposed a $Pt_3Sn(111)$ surface to CO and O_2 at different compositions and temperatures. In paper II we instead used Sn/Pt surface alloys and exposed them to CO and O_2. This enabled us to control the spread of the tin oxides formed, and to compare the activity of the platinum-tin surfaces to that of pure platinum. We could also study the role of edge sites by using two different platinum crystals: A flat Pt(111) and a terraced Pt(223), addressing the materials gap. In paper III we exposed the Sn/Pt surface alloys of paper II to higher pressures of CO and O_2, which was possible using a different experimental technique, XAS, than in papers I and II (XPS), addressing the pressure gap. Papers I, II, and III focused on operando measurements (while the reaction was taking place) of the platinum-tin surfaces. Paper IV dealt with preparing the $Pt_3Sn(111)$ surface in a way that is useful for surface science. Papers V and VI are detailed ultra-high vacuum studies of one of the unique tin oxides phases that form on platinum-tin surface. Thus our work has been split between gaining a fundamental understanding of the tin oxides that form on platinum-tin, and studying platinum-tin during reaction conditions.

This thesis is written so as to give an introduction to the included research papers, starting from the very beginning. I hope to give a reader an image of what catalytic materials are (in particular platinum-tin), how they behave and why, what information we could extract about these materials through experiments and how those experiments work. I will start by explaining what catalysis is, what makes it work, what it can and cannot do. I will also talk a little about the CO oxidation reaction in general. I will then explain what materials are, what makes the surfaces of materials special, and then thin films and their properties as they are the centre of the fields of surface science and catalysis. After this general introduction to the relevant fields of science, I will give the background to the material that I have studied: platinum-tin. Both platinum and tin have interesting properties and applications, but it is when they are alloyed that they have attracted the most attention as a catalyst. The mixing of these elements also makes complex surface structures possible, which have also attracted considerable interest. Platinum-tin has been used and studied for the oxidation of CO extensively in the past, and the last part of the scientific introduction will be spent explaining the previous work done on CO oxidation over platinum-tin. After this scientific introduction, I will explain the experimental techniques that we used in our papers. Also here, I want to start from the beginning to give the reader a fundamental idea of how the techniques work from a physical point of view. I will start by talking about the particles we use to extract information about the materials: electrons and photons and how they are generated. The main experimental techniques we have used can be broadly grouped in three categories: Spectroscopy, diffraction, and microscopy. They will have a part each. Two short sections at the end will introduce computational techniques we have relied on, and mass spectrometry. This is the technique we use to measure the gas composition above our samples, and is instrumental for saying something about the catalytic activity of our samples.

Chapter 2

Catalysis

In the introduction I lauded the filed of catalysis as perhaps the most significant one during the last century. Here I will introduce the field of catalysis and the fundamental physical processes behind it, how catalysis is studied, and finally introduce the CO oxidation reaction. In one sentence, a catalyst is a material that accelerates a chemical reaction without being consumed in the reaction [23]. This description may not sound very impressive, but the consequences are far-reaching. The accelerated rate makes it possible to run reactions at lower temperatures and pressures, which is an economical gain, but can also make the difference between being able to produce a chemical at all or not. The conditions that would be required to run a certain reaction without a catalyst could be too extreme (or expensive) to reach from an engineering perspective, or the desired product may not even survive them. What's more, the molecules used as reactants for the reaction can often combine to produce a multitude of products, not just the desired product. A catalyst can selectively accelerate only the reaction path leading to the desired product, reducing waste and by-products. The rate at which a catalyst accelerates a reaction (activity), and the ratio of desired to non-desired product (selectivity) are key attributes of any catalyst. A biological example of a catalyst are enzymes, which are bio-molecules that build or break down molecules. Thanks to enzymes the complex and specific molecules we depend on can be produced in the lukewarm confines of our bodies. In a way, catalysis is a cornerstone for (complex) life itself. Catalysts can be classified as homogeneous catalysts, in which case the catalyst is completely dispersed in the reactants on a molecular level (like enzymes in a solution), and heterogeneous catalysts, that are solid materials where only the surface interact with the reactants. The chemical reaction can be driven thermally or electrochemically. I will only discuss heterogeneous, thermal catalysts in this thesis.

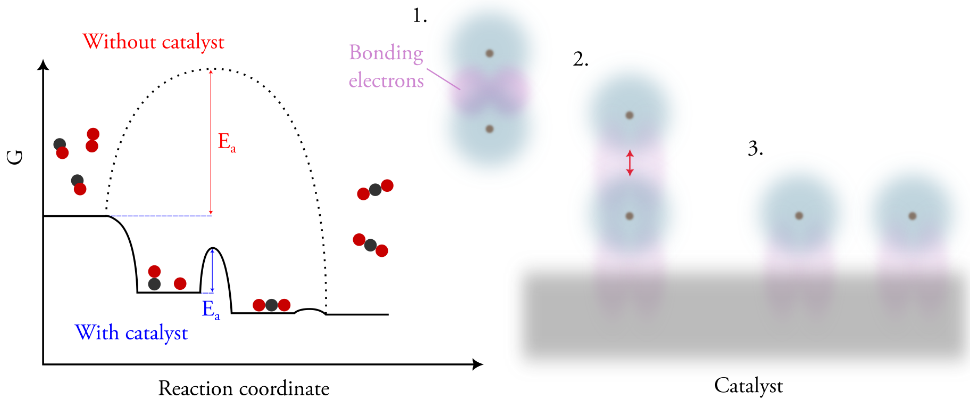

Figure 2.1: The principle behind catalysis. Left shows how a catalyst can lower the reaction barrier for a catalytic reaction, in this case CO and O_2 reacting to CO_2. Right shows how a catalyst surface facilitates the splitting of a diatomic molecule through interacting with the electrons holding the molecule together.

1 Fundamental concepts

A catalyst can accelerate the rate of a reaction, but not drive it. For a chemical reaction to occur, there must be a decrease in Gibb's free energy going from the reactants to the product. Gibb's free energy (G) is defined by [22] $G = E - TS + pV$, where E is the energy, T the temperature, S the entropy, p the pressure and V the volume. If the temperature, pressure and volume are constant, we can see that whether the reaction will occur or not depends on the energy and entropy of the reactants and the product. It is intuitive that molecule(s) can decay to a state with lower energy, but as we can see it is possible to produce a product with higher energy if the entropy increase is high enough. The entropy is a quantity that describes the number of available states of a system, and is a quantity that is always increasing (for an isolated system, according to the second law of thermodynamics [22]). A "state" can be the ways a molecule can move, rotate and vibrate, for example. The number of available states for an ensemble of molecules can be affected by, for example, the pressure and temperature in the reactor, and sometime high pressures are needed to make the reaction entropically favourable. An example is the Haber-Bosch process, where three hydrogen molecules and one nitrogen molecule become two ammonia molecules: going from four to two molecules is only favourable at pressures above 100 bar.

A catalyst increases the rate of a reaction by decreasing the barriers the molecules need to overcome to reach their new state. Such a barrier could for example be an oxygen molecule splitting apart into its two constituent atoms (which costs energy) before one of the oxygen atoms react with some other molecule. A catalyst can lower the energy cost required for this splitting by weakening the bond between the atoms in the molecule. The atoms in a molecule are held together by the valence electrons, usually occupying the space between the atoms in the molecule. When a molecule comes into contact with the catalyst, these bonding electrons can be partially donated to the catalyst material, lowering the electron density in the molecule and weakening the bond they participate in. This is the fundamental process by which catalysts work, and is illustrated in the right part of Figure 2.1.

In order for for a catalyst to work, it needs to bind the reactant molecules to its surface. To do this there needs to be available states near the Fermi level of the material where the electrons from the reactant molecules can go. For this reason the electronic band structure of the material near the Fermi energy is the most important quality of a good catalyst. Many catalysts are transition metals, and their activity can be understood using the d-band model. The d-band contains a large number of states with similar energy, and for transition metals this band is at the Fermi level. Elements like scandium and yttrium have nearly empty d-bands while copper, silver and gold have a fully occupied d-bands. Metals with a full d-band have weaker interactions with adsorbed molecules, as there are so few available states that the electrons from the molecule can occupy. This is why, for example, gold is inert and resistant to oxidation. Metals that have a half-filled d-band, like iron, have a large number of available states and interact strongly with adsorbed molecules. In order to have an ongoing reaction, all reactants need to be able to adsorb on the surface and the product needs to desorb from the surface to make place for new reactant molecules. For this reason many catalysts are materials that do not bind the reactants (or products) too tightly or too loosely. This is summed up in Sabatier's principle [23], saying that the optimal rate for a catalytic reaction is a function of the absorption energy of the molecule. The result is a volcano-like plot where elements with lowly filled d-bands have low activity, elements with an "appropriate" level of filling a high activity, and elements with highly filled d-bands have low activity. What an "appropriate" level of filling is depends on the reaction in question. When one of the reactants binds too strongly to the surface it will block adsorption of the other reactants and no reaction can take place. This problem is called poisoning. There are three fundamental mechanisms by which a product molecule can form over a catalyst. The Langmuir-Hinshelwood mechanism involve several reactants that both adsorb on the surface, meet, react, and desorb. This is the mechanism discussed so far. A reactant can also adsorb on a surface, react with something from the material itself (like oxygen from an oxide on the surface), form the product and desorb. This is the Mars van-Krevelen mechanism. Finally, a reactant molecule can react with something on the surface directly from the gas phase without first adsorbing on the surface, this is the Eley-Rideal mechanism.

2 Real systems and model systems

Real, industrial catalysts typically consist of nano particles dispersed on a porous oxide support. This is done to maximize the surface area of the catalyst, and to disperse it in the reactor. The pressures of the gases in the reactor can be from atmospheric pressures up to several hundred atmospheres. The nano particles can display several surface truncations, edge sites, and defects. The surface area may also change during operation, for example through sintering, where smaller particles fuse into larger ones. What oxide support is used and how it interacts with the nano ,particles and/or reactants can also have an effect on the activity. This makes for a very complicated system that is difficult to study. The activity of the catalyst in the reactor is relatively straightforward to measure, but knowing what caused the activity is very difficult, as there is a large number of possible sites that could catalyse the reaction. Often a minority site, such as the edge sites, can be responsible for the majority of the catalytic activity. In order to gain a more fundamental understanding of the catalytic processes, simplified systems are often studied instead of the real catalyst.

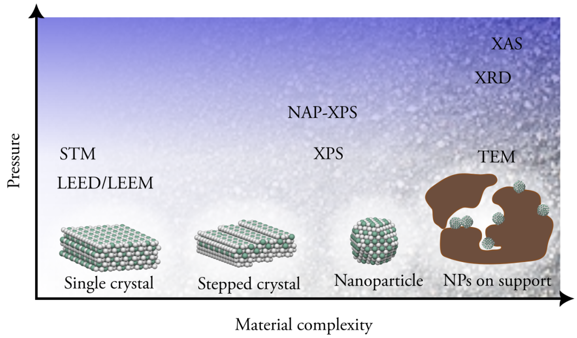

Figure 2.2: The materials and pressure gap.

The problem of the great diversity of surface sites in a real catalyst can be handled by creating samples that only contain one or a few of these sites and study them. A common way to do this is to use single crystal surfaces, which have a single surface truncation and a much lower edge and defect density than a nano particle. Studying these simplified catalyst surfaces offers greater insights into the processes that occur on the surface, but introduces the question whether what is seen on the simplified sample is what is responsible for the activity seen for the real catalyst. This problem is called the materials gap. Many useful experimental techniques cannot tolerate high pressures, and some require vacuum conditions. In order to use them, catalysts are often studied at pressures from UHV conditions ($\sim 10^{-9}$mbar) up to about 1 mbar. That catalysts are studied at pressures much lower than those used in industrial catalysts is called the pressure gap. For some applications, for example when the reaction of interest happens at low partial pressures, using mbar pressures can be more directly relevant.

3 CO oxidation

The catalytic reaction studied in this thesis is the CO oxidation reaction, it will be briefly described here. The catalytic reaction proceeds by CO adsorbing on the surface, O_2 adsorbing and dissociating on the surface, CO and O combining into CO_2 which then desorbs. The steps can be expressed as:

$$\begin{array}{lrl} 1) & CO + * \overset{k_1}{\rightleftharpoons} & CO* \\ 2) & O_2 + 2* \overset{k_2}{\rightleftharpoons} & 2\,O* \\ 3) & CO *{}^{+} O* \overset{k_3}{\rightleftharpoons} & CO_2* \\ 4) & CO_2* \overset{k_4}{\rightleftharpoons} & CO_2 \end{array}$$

where $*$ denotes an absorption site on the surface and a chemical symbol followed by $*$ a molecule adsorbed on the surface. The Formation of CO_2* from adsorbed $CO*$ and $O*$ (3) is the bottleneck of the reaction. CO_2 binds very weakly to most surfaces and quickly desorbs, CO binds strongly and quickly, and O_2 is easily dissociated by the catalyst. Without the catalyst the splitting of the O_2 molecule (in the gas phase, then) would be the limiting step, needing about 500 kJ mol^{-1}. The energy required for $CO*$ and $O*$ to react on the catalyst surface is instead about 100 kJ mol^{-1}. The energy gained from going from CO + $\frac{1}{2}$ O $_2$ to CO_2 is about 285 kJ mol^{-1}. CO is a reactive molecule, and its strong bonding to the surface can be a problem. At lower temperatures the catalyst surface risks becoming covered by CO, leaving no sites where O_2 can adsorb and dissociate. The surface is poisoned by CO. Often one can increase the CO desorption rate by raising the temperature to alleviate the problem, but this is sometimes not possible. The temperatures required could be unreachable if the reaction takes place in a liquid (with a certain boiling point) or undesired reactions may start taking place in the reactor. One example is the cleaning of CO from streams of hydrogen gas. Even small amounts (ppm) of CO can poison the catalyst intended for the reaction involving the hydrogen, so any CO in the gas stream needs to be removed. One needs a catalyst that can oxidise only the CO at a low temperature to avoid also oxidising the hydrogen (this is called preferential oxidation in hydrogen, PROX). For this and other reasons, catalysts that can oxidise CO at mild conditions are very sought after.

Chapter 3

Crystals and crystal surfaces

At the centre of this thesis work is the material platinum-tin and the structures that can form on its surface. In this chapter, materials science will be introduced in a general way, explaining what makes up solid matter and the concepts that are important for understanding the rest of the thesis work. First, a brief description of the atom will be given as all matter is made up from atoms, and it will aid in understanding some of the experimental techniques (as well as catalysis). Then, crystal structures and the structure of solids will be described, followed by surface structures and the unique phases that can form on surfaces.

The atom is the fundamental building block of the vast majority of materials. The electrons should be considered as having a probability density that extends over the size of the atom (rather than as small balls orbiting the nucleus, which is how they are often depicted). The probability density determines how probable it is that the electron will be detected in that point, it can be thought of as a ”cloud” of presence for the electron. The electrons in the atom arrange themselves in so-called shells with different energies associated with them. The shells are numbered from one (1) and upward. Some of the electrons in a shell can have angular momentum as well. They are named as s-electrons if they have no angular momentum, p-electrons if they have one unit of angular momentum, d for two units, f for three units (angular momentum is quantised). This nomenclature shows up when discussing for example the XPS technique (the core levels are named 1 s, 3 d etc.). The shapes of the electron clouds are often not spherically symmetric but has preferred directions where the density is higher. With this image of the atom in our minds, let us move on to solids.

1 Crystals

When atoms are put together, they can form solids. This happens because the outermost electrons in the atoms gets affected by the potential from the neighbouring atoms, and these electrons then bind the atoms in the solid together in a rigid structure. When the outermost electrons gets affected by the other atoms, the discrete energy levels they would have in an isolated atom widen to form energy bands. For example, the electron energies in a solid that originates from d electrons in the atom, is called called the d-band. The highest shells in the solid will form bands in this way while the inner, core, shells will stay discrete.

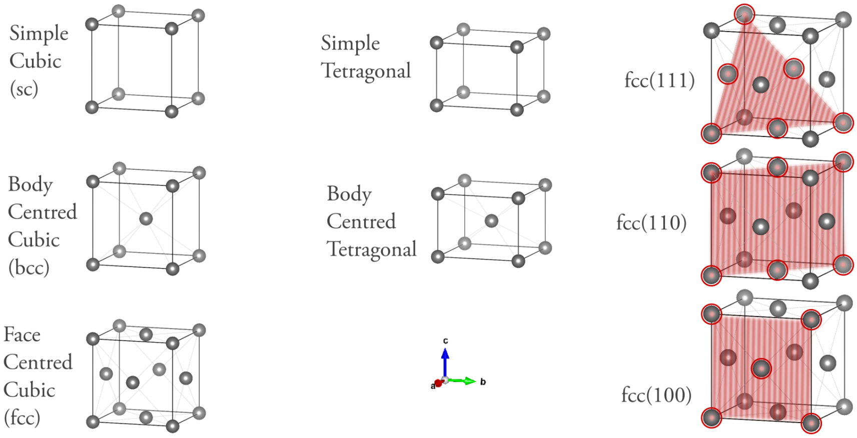

Figure 3.1: Crystal structures and planes. Left shows three common cubic unit cells, middle shows two tetragonal unit cells, and right shows the three simplest planes for the fcc unit cell.

The materials that were studied in this thesis work are crystalline solids, where the atoms arrange themselves in a periodically repeating pattern [63]. The repeated unit can be a single atom or a cluster of atoms, arranged in a unit cell. The unit cell is described by three vectors $\mathbf{a_x}$ spanning out the cell as $\mathbf{R} = \mathbf{x} \cdot \mathbf{a}_1 + \mathbf{y} \cdot \mathbf{a}_2 + \mathbf{z} \cdot \mathbf{a}_3$. If the unit cell is the smallest possible cell that can describe the solid it is called a primitive unit cell. Often, it is convenient to work with cells that are cubic or tetragonal even if they are not primitive. Common unit cells are the simple cubic (sc), simple tetragonal, body centred cubic (bcc), body centred tetragonal, and face centred cubic (fcc), which are displayed in Figure 3.1.

To define planes and surfaces in solids, one makes a cut in the unit cell. The planes are named by their Miller indices, which are the points where the plane intersects the unit cell axes $\mathbf{a}_1$, $\mathbf{a}_2$, $\mathbf{a}_3$. The indices h, k and l, and are defined so that the intersect with the unit cells axes should be $(\mathbf{a}_1/\mathbf{h}, \mathbf{a}_2/\mathbf{k}, \mathbf{a}_3/\mathbf{l})$, so the intersects are fractions of the unit vectors $\mathbf{a}_1$, $\mathbf{a}_2$, $\mathbf{a}_3$ (for example, $l = 2$ means the intersect happens half-way along $\mathbf{a}_3$). The three simplest planes for a cubic cell are shown to the right in Figure 3.1. For clarity, the atoms included in the plane have been circled in red.

2 Surfaces

The surfaces (or surface truncations, as they are also called) that can form on a solid is described by the planes defined by the miller indices. For example, the fcc (111) surface contains the atoms in the plane in Figure 3.1, top right, and is displayed in Figure 3.2 (top right). The atoms in a solid lower their energy by being close to their neighbours, and atoms on the surface have fewer neighbours than those in the bulk. Therefore, there is a cost in energy for making a surface on a solid. The energy cost is usually different depending on how the crystal is cut, and is typically lower for the surfaces where the atoms are packed more closely together. For fcc materials the (111) surface is the most close packed and has the lowest energy. For that reason, it is a common surface truncation.

It is useful to define a number of sites on the fcc (111) surface, as molecules often prefer to occupy specific sites on a surface. Top sites are directly on top of one of the atoms in the surface layer, bridge sites are in between two topmost atoms, and hollow sites are in the middle of three surface atoms. Depending on if there is an atom directly below the hollow the sites are named differently. The site is called hcp-hollow is there is an atom directly below the hollow (in layer B) and fcc-hollow is the atom below is one more layer below (layer C). Besides these sites, defects and inhomogeneities may also be present on a surface. One of the most common such sites are edge sites. The ideal fcc (111) surface is layered atomically flat, but in practice it is not possible to prepare a surface that is this flat on a macroscopic scale (larger than ∼μm). On the atomic level, this unevenness will form a terraced structure. An example of a terraced structure is the fcc (223) surface in Figure 3.2. The flat sections have the same structure as fcc (111).

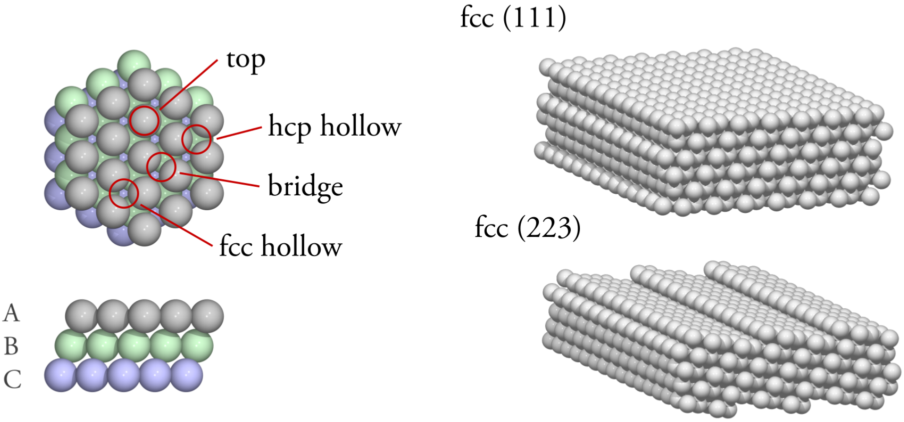

Figure 3.2: Crystal surfaces. Left: different sites on the fcc (111) surface (top) and the layers of the fcc (111) surface (bottom). Right: two fcc surfaces used in this thesis work, fcc (111) (top) and fcc (223) (bottom).

3 Thin films and 2D materials

The surface of a material is a unique environment which can influence the structure and chemistry of materials confined to the surface region. For example, the energy cost of being at the surface varies depending on the element. A solid containing more than one element may re-arrange from its bulk composition so that the element with the lowest surface energy gets enriched in the surface layer. This is what happens for platinum-tin surfaces, which will be described in section 4. Some oxides bind strongly to metals, more strongly than they bind to the rest of the oxide. This Strong Metal Support Interaction (SMSI) was discovered when the oxide support for metal nanoparticles grew and encapsulated the metal, inactivating it [110, 109]. The properties of the 2D oxide films that grow in this manner are often different to that of the bulk oxide. Strain induced by lattice mismatch between oxide and metal, electronic effects, unique atomic structure, and chemical reactions occurring on these films can all give them unique behaviour [78]. The 2D oxide films often contain defects and vacancies as well, which are particularly important for catalysis [92]. Through the formation of these unique oxide structures, a combined metal-oxide surface can become catalytically active for reactions where the metal or oxide alone are not [92, 107, 108]. The prospect of finding new catalysts made from otherwise well-known elements has ignited a great interest in these ultra-thin oxide materials.

4 Platinum-tin

Now we will turn to the topic of this thesis work: platinum-tin. As a catalyst, it is used for a range of reactions, like dehydrogenation of carbon compounds [50, 25], thermal oxidation of CO [99, 98, 3, 77], and electro-oxidation alcohols [67, 59, 30, 118, 117] and CO [42, 43, 106, 105]. The addition of tin to the platinum improves the activity relative pure platinum for several of these reactions. For providing some background and context, I will first introduce platinum as a catalyst followed by a description of tin and its oxides. Then the material properties of platinum-tin will be described before its function as a catalyst will finally be described. Platinum-tin has many uses, but I will focus on CO oxidation, as that is the topic of most of the included research papers.

Platinum

The periodic table's 78:th element, platinum, is most famous for being an excellent catalyst, as well as being very expensive[1]. It is a transition metal with an fcc structure with a lattice constant of 3.92 Å, with (111) as the most stable surface (see Figure 3.2 for an example), and a melting point of 1772°C [63]. Platinum is in group 10 in the periodic table, meaning that it has a nearly filled d-band (9/10 electrons). This makes it more noble than most metals but not as noble as, for example, gold (the 79:th element). The nearly filled d-band is what gives platinum its properties as a catalyst. Platinum immediately dissociates O_2 when it gets close enough to the surface, and the resulting O atoms bind to the surface. To dissociate O_2, two adjacent sites on the surface are required. It is also efficient at dissociating H_2. Platinum also adsorbs CO. Early work on the catalytic reactions of H_2, O_2 and CO over platinum surfaces was done by Irving Langmuir [68, 69]. He found that CO poisoned the platinum surface for CO oxidation at temperatures below about 230°C (500°K) by blocking sites for O_2 dissociation. CO prefers to bond on certain sites on the platinum surface. On Pt(111) top and bridge sites are preferred, while stepped surfaces have additional adsorption sites on atoms in the steps [55]. When reacting with an adsorbed O atom, the CO moves slightly out of its top site position which increases the repulsion between the CO and the O (sitting in a hollow site). The O is pushed into a bridge site after which it reacts with the CO and leaves the surface as CO_2 [35]. CO_2 is weakly bound to the surface and quickly desorbs once formed. For the reaction to take place the temperature needs to be high enough to keep the CO coverage low enough to enable sites for O_2 dissociation. High temperatures are problematic for certain applications, having led a search for additions and alterations to make more CO tolerant platinum based catalysts. One of them is tin.

---

[1] The price of platinum has been about 30'000 EUR/kg over the last few years [87], to be compared with gold at about 40'000 EUR/kg in the same period (although the price of gold fluctuates a lot, and is at the time of writing closer to 70'000 EUR/kg.

Tin and its oxides

Tin is the 50:th element of the periodic table, the same group as carbon, silicon, germanium, and lead[2]. It is soft, has a body centered tetragonal crystal structure (with lattice constants of 5.83 Å and 3.18 Å), and a melting point of 232°C [63]. The d band is filled, and the valence electrons consist of two 5s and two 5p electrons. It has long been used for alloying with other metals, for example with copper to make bronze in the ancient times. It is not noble like platinum, and is readily oxidized to either Sn^{2+} or Sn^{4+}, of which the latter is more stable. The energy difference between the two states is not so large, which affects the structure and properties of tin compounds. Tin can form several forms of oxide, and I will describe them briefly here.

Tin forms primarily two types of oxides: stannous oxide ($Sn^{2+}O^{2-}$) and stannic oxide ($Sn^{4+}O_2^{2-}$) (see ref [14] for a review). Stannic oxide is found naturally, for example in the mineral Cassiterite (which is the main ore for tin production), and is more stable than the less oxidized stannous oxide. Stannic oxide has a tetragonal unit cell with a rutile structure, the tin atoms are sixfold coordinated to oxygen. For bulk stannic oxide, the (110) surface is the most stable. When stannic oxide grows on Pt(111), the (101) surface is favoured as the lattice mismatch between SnO_2(101) and Pt(111) is lower than for SnO_2(110). On the SnO_2(101) surface the topmost oxygen atoms are loosely bound, and the surface layer easily reduces to Sn^{2+}. In stannous oxide (SnO) the 5p electrons participate in the bond with oxygen, while the 5s electrons are left with the tin. This contributes to the formation of a layered structure, where the 5s electrons cause repulsion between the layers. The unit cell is tetragonal with a litharge structure, and the tin atoms are fourfold coordinated to oxygen. Tin oxides are primarily used for transparent conductors, gas sensing applications, and also as catalysts. The dual valency Sn^{2+}/Sn^{4+} (or Sn(II)/Sn(IV)) is believed to be important for these applications.

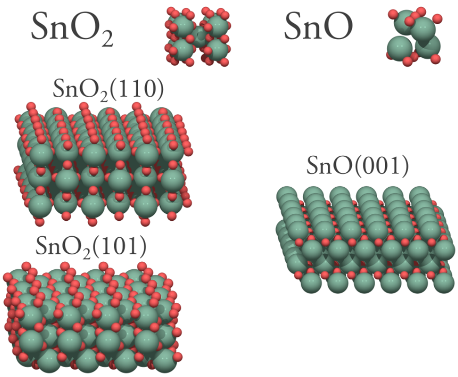

Figure 3.3: SnO_2 and SnO, their unit cells and most common surfaces. The SnO_2 surfaces exist in oxygen terminated and tin terminated version.

---

[2] It's the first metal in that group.

4.1 Properties of platinum-tin

When mixed, it is energetically favoured for platinum and tin to form alloys and intermetallic compounds [34] The most commonly formed is the Pt_3Sn alloy, which has a fcc unit cell with tin on the corners and platinum at the faces (see Figure 3.4). The structure is like that of platinum, but with some of the platinum atoms substituted by tin. Tin atoms are slightly larger than platinum atoms, which causes the lattice constant of Pt_3Sn to expand slightly relative platinum to 4.00 Å. The melting point is lower than for platinum, but still relatively high at 1404°C. When tin is added to platinum, the band structure of the material changes. The platinum d-band hybridises with Pt 6s and 6p states as well as Sn 5p states [103], which leads to a lower density of states at the Fermi level and a downward shift of the d-band [120]. This change of the electronic structure has consequences for how molecules bind to the platinum-tin surfaces.

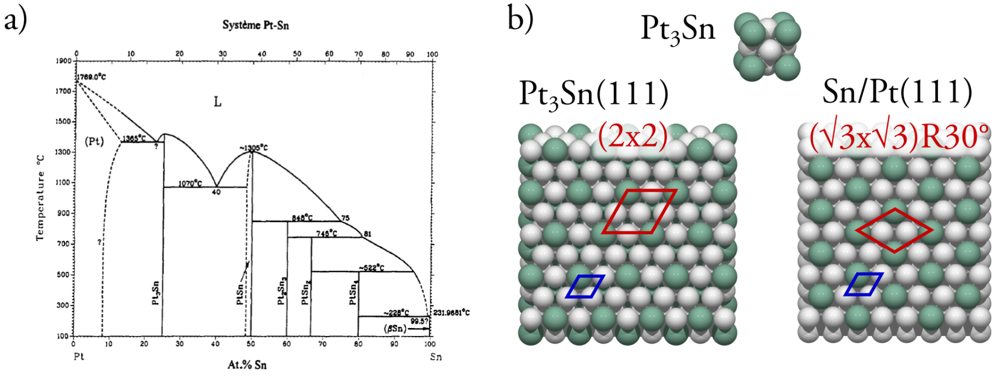

Figure 3.4: a) The phase diagram of platinum-tin. From Ref. [34]. b) Top shows the Pt_3Sn unit cell, left shows the bulk truncated $Pt_3Sn(111)$ surface, and right shows the tin enriched Sn/Pt(111) surface.

4.2 Platinum-tin surfaces

When cutting Pt_3Sn along the (111) plane, it results in a surface similar to the Pt(111) surface, but where the tin atoms form a (2×2) unit cell on top. A model of this surface is shown to the left in Figure 3.4. The structures that form on platinum-tin surfaces are named after how they compare to the corresponding platinum surface (so since the platinum-tin surface cell has the same shape as the platinum cell but the sides are about twice as long it is named the (2×2) surface). This truncation is the favoured one, and does not normally reconstruct [47, 46, 5, 113]. However, a surface reconstruction with a $(\sqrt{3} \times \sqrt{3})R30°$ structure can form on the $Pt_3Sn(111)$ surface. It has a tin enriched surface region (Pt_2Sn) and a sub-surface region that is depleted of tin [6, 21, 66]. It is displayed in Figure 3.4 b), right. On the $Pt_3Sn(111)$ surface it forms because of preferential sputtering of tin (more tin than platinum is removed during the cleaning process of the Pt_3Sn single crystal), leading to tin depletion in the surface layer [26]. The mobility of tin in the crystal is also limited (to about the two outermost layers) at temperatures below about 700°C, hindering replenishment of tin to the surface from the bulk [26]. It is in other words a tin over-layer structure on Pt(111).

Tin surface alloys can also be formed on the Pt(111) single crystal surface by deposition of tin followed by annealing [86, 83]. The surface alloy is stabilised by the minimisation of surface free energy of the system, as tin has lower surface energy than platinum [10]. The structure formed depends on the coverage of tin, with lower coverage (up to 1 mono-layer (ML)) leading to the $(\sqrt{3} \times \sqrt{3})$R30° structure and higher coverage (a few ML) leading to formation of a layer of the bulk truncated Pt_3Sn(111) (2×2) structure after annealing to about 300°C [37, 38]. The tin atoms in the surface alloys are slightly protruding from the Pt(111) surface (by about 0.2 Å) [83, 7]. The alloying of platinum and tin influences the core level binding energies by shifting them upward by 0.4 eV and 0.3 eV respectively for Pt 4f and Sn 3d [86, 37], making it possible to distinguish the pure metals from the alloy with for example XPS. The addition of the tin changes the nature of the adsorption sites available on the surfaces. On the $(\sqrt{3} \times \sqrt{3})$R30° surface, all hollow sites now contain a tin atom. On the (2×2) surface fcc hollow sites also contain one tin atom, while the hcp hollow sites still have three platinum atoms, but have a tin atom directly under it. The change in electronic structure also has an effect on the adsorption energies of molecules for the different adsorption sites on the platinum-tin surfaces.

Many molecules bind to platinum-tin, here I will focus on CO and O_2. CO binds to the Pt_3Sn(111) (2×2) and $(\sqrt{3} \times \sqrt{3})$R30° Sn/Pt(111) surfaces just as it does on platinum, but the adsorption energies are lower. In temperature programmed desorption (TPD) studies the desorption temperature is lowered by about 50-100°C for PtSn surfaces relative platinum [85, 45], which corresponds to a lowering of the adsorption energy of about 20 kJ mol^{-1} [93]. The effect and can be explained by the lowering of the platinum d-band, which decreases the overlap of the d-band with the states in the CO molecule involved in the bond [93]. Density functional theory (DFT) calculations of the bonding of CO to platinum-tin supports the lower adsorption energies relative platinum[70, 100, 72, 33, 115, 61], as do measurements [33, 115, 106]. Band structure measurements using angle resolved resolved photo emission spectroscopy by Jung *et al.* [61] provided a direct view of how the d-band participates less in the bonding with CO for Pt_3Sn than for Pt. Contrary to on Pt(111), on-top and hollow sites are both about equally favoured for CO adsorption on Pt_3Sn(111) [100, 72, 33].

Tin has a higher affinity toward oxygen than platinum, and what happens when the platinum-tin surface is exposed to oxygen (at sufficient temperatures) is that the tin oxidises [52, 51, 112]. The adsorption energy for O_2 on platinum-tin is lowered relative platinum, and no dissociative adsorption typical for platinum was seen in early surface science studies of O_2 on Pt_3Sn(111) surfaces [85]. Exposure to O_2 at ~0.02 mbar at ~100°C oxidises the

(2×2) and $(\sqrt{3} \times \sqrt{3})$R30° surfaces, with the (2×2) surface oxidising faster than the $(\sqrt{3} \times \sqrt{3})$R30° surface [58] (the same effect was seen when oxidising with O_3 at lower pressures [96]). Presence of threefold platinum hollow sites on the (2×2) surface (lacking on the $\sqrt{3}$ surface) are probably important for the initial dissociation of O_2, as are minority domains of pure platinum. The O atom itself binds as strongly to $Pt_3Sn(111)$ surface as to the Pt(111) [116, 31].

The oxides that form on the $Pt_3Sn(111)$ and Sn/Pt(111) surfaces turn out to have complex structures and behaviours, and have received some academic attention over the last few decades. Batzill *et al.* oxidised the (2×2) and $(\sqrt{3} \times \sqrt{3})$R30° surfaces with NO_2 at 130°C followed by annealing, which revealed several new oxide structures [11]. Flash annealing to 600°C resulted in nano islands of SnO_x, which ordered into a (5×5) pattern if the procedure was repeated a few times. Annealing at 600°C for several minutes resulted in a wetting surface oxide with a (4×4) periodicity. X-ray photo emission spectroscopy yielded binding energies for the tin in the oxide intermediate between metallic tin and Sn^{2+} (the same binding energy was also seen in the study using O_2 mentioned earlier [58]). It indicated that the surface oxide was less oxidized than the bulk tin oxides (similar intermediate binding energies was seen earlier on oxides formed on Pd_3Sn [94]). The (4×4) oxide is quite resistant to reduction by H_2 if it is well ordered [65]. The (4×4) oxide can be formed also by O_2 exposure at 10^{-6}mbar pressures, and was found to be a monolayer through XPD [53, 4]. The composition was finally calculated using a global structure search to be $Sn_{11}O_{12}$ with a structure stabilised by bonding with the $Pt_3Sn(111)$ substrate [75].

When oxidising the $Pt_3Sn(111)$ surface to form the (4×4) surface oxide, yet another structure was found which has a "streaky" (2×2) diffraction pattern [53]. It is an oxide related to the (4×4) oxide, and its structure is presented in paper v. It is referred to as the $(2m \times 2n)$ oxide, from its structure. It consist of domains of 2D oxide with a striped structure, with varying periodicity between the stripes (given by n) as well as some periodic structures going along the stripes (given by m). STM images of the two phases are shown in Figure 3.5. The growth conditions and further characterisation is included in paper vi. The $(2m \times 2n)$ oxide is easily reduced to the (4×4) oxide by CO, making it an interesting oxide phase for CO oxidation.

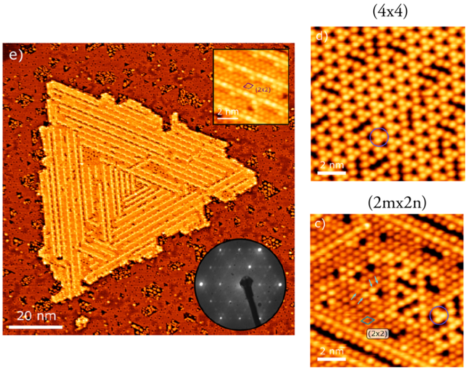

Figure 3.5: STM images of the surface tin oxides. Left: island with a mixture of the two oxides and LEED image (inset), right: $Sn_{11}O_{12}$ (4×4) oxide (top) and Sn_3O_4 $(2m \times 2n)$ oxide (bottom), from paper v.

Some tin oxides on the Pt(111) surface have a higher oxidation state than the (4×4) and $(2m \times 2n)$ surface oxides just discussed. One example is the SnO_x nano islands in Ref. [11]. They are more oxygen rich than the (4×4) oxide (and can be formed by oxidising the (4×4)), but appear weakly ordered [12, 13]. The island nature (rather than a film) and ordering into lines of islands and finally a (5×5) pattern was suggested to be due to a stress relief mechanism. Yet another structure was sometimes formed when re-oxidising the nano islands: an incommensurate, ordered, SnO_x film. The oxygen content was similar to that of the nano islands, and the unit cell is close to the SnO_2(101) cell, suggesting structural similarity.

Even more oxidized tin oxide films can be formed on Pt(111) by depositing tin in an NO_2 atmosphere at 330°C [15]. Multi-layered tin oxide films formed, which grew by first forming a wetting mono layer oxide film (the (4×4) phase and related features) and then multi-layered oxide (Stranksi-Krastanov growth mode). The surface truncation was not (110) (the most stable for bulk SnO_2), but the (101) truncation which is otherwise not very favourable. The explanation is that the SnO_2(101) unit cell matches very well with the Pt(111) substrate, contrary to the SnO_2(110) and SnO_2(100) unit cells which otherwise have lower free energy. The crystallites also showed XPS binding energies close to (but slightly lower than) than of bulk $Sn^{4+}O_2$. In paper III, we saw signs similar growth modes when exposing Sn/Pt surface alloys to partial pressures of $\sim$50 mbar O_2 while heating: the XANES spectra at temperatures up to about 100°C matched with simulated spectra of the (4×4) and $(2m \times 2n)$ oxides followed by SnO_2 at temperatures above 150°C.

In summary, the platinum-tin surface is complex. The strong bonding between platinum and tin, the propensity to form surface alloys, the dual Sn^{2+}/Sn^{4+} valency of tin and its effect on the oxides it can form results in multitude of different structures, where bonding between metal and oxide is often important. So far we have only considered how platinum-tin interacts with carbon monoxide or oxygen separately, but platinum-tin is a catalyst and we want to know how it interacts with these molecules under reaction conditions.

4.3 CO oxidation over Platinum-tin

The ability of platinum-tin to oxidise CO in electrochemical environments has been extensively studied due to its importance for fuel cell technology [42, 43, 41, 106, 105, 48, 49, 88, 3, 91, 72, 73]. The potential required for electro-oxidation of CO on platinum-tin is much lower than on platinum. The findings revolve around the adsorption energy of CO on the platinum-tin surface, in particular on Pt_3Sn(111), and the ability of tin to adsorb or dissociate water. The reaction proceeds by bifunctional mechanism with platinum providing the CO and tin the OH.

Platinum-tin catalysts have also been shown to be effective for CO oxidation in the gas phase [39, 99, 2, 98, 102, 76, 77]. The apparent activation energy for CO oxidation is lowered from 133 kJ mol^{-1} on platinum [76] to about 30 kJ mol^{-1} on platinum-tin [76, 77], and the reaction order for O_2 changes from about 1 for platinum to values between 0.5 to 0 depending on the O_2:CO ratio [76] (0.5 if there is less O_2 than CO, 0 if thre is a great excess of O_2). This shows that the reaction over platinum-tin is not limited by the O_2 adsorption like it is on platinum. Instead, O_2 dissociation is limiting at low O_2 pressures, while at higher pressures oxygen is available in excess and does not limit the reaction. The down shifting of the d-band of platinum on alloying with tin, and the resulting lowered CO adsorption energy, is seen also for platinum-tin nanoparticles in the gas phase [102]. Even in reducing conditions, however, the tin is often not completely metallic or alloyed, but in an Sn(II) state [19]. The Sn(II) oxides have been identified with increased activity in several studies of CO oxidation over platinum-tin nanoparticles [39, 2, 98, 76, 77]. The Sn(II)-Sn(0) redox pair is proposed to be responsible for the activity in the most recent studies [76, 77].

Single crystal surface science studies have also provided insight into the CO oxidation reaction over platinum-tin surfaces [60, 8, 9, 33, 32]. This is also the topic of papers I, II, and III. Temperature programmed desorption (TPD) on Sn(II) oxide islands on Pt(111) resulted in CO_2 production and reduction of tin for small, dispersed islands through a reduction of the tin from Sn(II) to Sn(0) [8]. A surface covered in tin oxide islands resulted in no CO_2, and the Sn(II) oxide transformed partially to Sn(0) and Sn(IV) (the (4×4) oxide behaved the same way). These changes were followed with Near Ambient Pressure XPS were the gradual reduction of the low coverage tin oxide was followed as was the rapid transformation of the covering tin oxide [9]. The transformation was attributed to a disproportionation reaction were CO drives the reaction $2\times$ Sn(II)O $\rightarrow$ Sn(IV)O_2 + Sn(0), but without reacting to CO_2. High Pressure STM also showed the high coverage Sn(II)O islands de-wetting to form clusters upon exposure to CO (the low coverage islands were unaffected). The experiments highlighted how the gas composition affects the structure and chemistry of the tin oxides that form when exposed to CO.

When we exposed a $Pt_3Sn(111)$ surface to CO and O_2 at ~1 mbar and heated stepwise in paper I, tin segregates from the alloy and starts oxidising at the same temperature as CO_2 starts forming. The oxide that forms depend on the gas composition over the surface with an oxygen rich (1:10 $CO:O_2$) mixture leading to wetting Sn(II) oxide and an even mixture (1:1) to clustered Sn(IV) oxide. The ability of CO to cause dewetting of Sn(II) oxides combined with a difference in activity of the covering oxide and the metallic surface resulted in self-sustained oscillations in the activity of the surface. On the Sn/Pt surfaces in paper II Sn(II) oxide formed in 1:1 $CO:O_2$. We saw reduction of the Sn oxides by CO during reaction conditions, and the reduction was completely dependent on presence of oxide edge sites. The strongest reduction of the oxides, followed by formation of Sn(IV) oxide and metallic tin, was seen on stepped surfaces, showing the importance of step and/or edge sites for this transformation. A covering Sn(II) layer is neither reduced nor further oxidised at any temperature. At higher pressures (~50 mbar) Sn(II) oxides form during CO oxidation conditions, which are not reduced as the temperature is increased, seen in paper III.

The oxide growth caused a gradual decrease in the rate of the CO oxidation reaction on the $Pt_3Sn(111)$ surface in paper I, showing that the oxide surface is less active than the metal in those conditions. The activity of the alloy surfaces in paper II were also more active at low temperatures than the oxidised surfaces at the same temperatures. The reduction of the Sn(II) oxides seen in paper II was not a major cause of the improved activity of the Sn/Pt surfaces relative Pt. Instead the activity was mainly attributed to alloy or small oxide clusters at lower temperatures and the Sn(II) oxide itself at higher temperatures. The rate of the reduction was substantial, however, and may be one of the contributing mechanisms of the CO oxidation reaction, but not the only one. The Sn(IV) and its reduction was not related to any improved activity.

In summary, on the single crystal Pt_3Sn and Sn/Pt surfaces we studied the tin always oxidised during CO oxidation conditions, with the gas composition having a big effect on which oxide formed. Fine details in the experimental conditions affect the gas composition and therefore the nature of the oxide formed, and whether it is reduced or not. The oxide edge sites are crucial for facile reduction of the oxides. There are good indications that the platinum-tin alloy contributes to the improved CO oxidation activity, when it is present. The tin oxides, however, also play a role in the oxidation of the CO. Identifying active sites and how significant they are for the overall rate of the reaction is difficult, but the Sn(II) oxide definitely seem more active than the Sn(IV) oxide, which agrees with previous works. At least some of this activity seems related to the Sn(II) oxide itself, rather than its edges.

Chapter 4

Methods

In order to understand the material systems that we are interested in better, we want to extract information from the materials themselves under as realistic conditions as possible. This is where experimental techniques come into the picture. Information that can be extracted from the surfaces we are interested in include the chemical states of the elements on the surface, the atomic structure of the surface, the morphology of the surface, what adsorbates are present and their coverage, which gases are present above the surface etc. Experiments have the advantage that they always provide information about reality, but sometimes they are not enough. Not every piece of information can be obtained through experiments, and experimental data can be difficult or expensive to produce, or difficult to interpret. Then theoretical methods can be helpful. They can be used to simulate atomic structures, or predict how experimental data should look like under certain conditions. The disadvantage is that for the complex systems we work with, one needs to make a number of approximations and assumptions about the system in order to calculate its properties. Those approximations and assumptions could of course be wrong, leading to results that have nothing to do with reality (to be fair, experiments also rely on assumptions for their interpretation, but if done right one can at least be sure that one studies something that exists, even if it would be too complex to understand). Together, experiments and theory are a powerful pair to unravel the behavior of materials. In this chapter the techniques used used in the papers will be described from a theoretical and practical point of view. Most of the experimental techniques used in this work use electrons or x-rays as probes to investigate the surface, I will briefly introduce them.

0.1 Electrons and x-rays as probes

Electrons are elementary particles with a wave-particle duality, making them useful for materials characterisation. Common techniques that utilise electrons are diffraction, microscopy and spectroscopy, examples of each will be described in the following sections. The wave nature of the electron was first discovered by de Broglie [28] in 1924, and the wavelength can be calculated by $\lambda = \frac{h}{m_e v} = \sqrt{\frac{h^2}{2m_e E}}$, where h is Planck's constant, m_e the electron mass and E the electron energy. For electrons of 25 eV the wavelength is about 2.5 Å (a typical inter-atomic distance), for 100 eV it is 1.2 Å (typical for LEED), and for 15 keV it is 0.1 Å (typical for RHEED). One of the main reasons to use electron based techniques is the ease at which one can produce and control electron beams. Typically, a tungsten filament or a conical tip of LaB_6 is heated to a few thousand degrees, which causes the electrons in the filament to have enough thermal energy to overcome the work function and escape the material. They can then be collected, accelerated, and controlled using electric fields. This works because electrons are charged, but the charge also introduces limitations: the mean free path of electrons in matter is very short (a few Å). Therefore, electron based techniques typically require ultra high vacuum conditions to work. On the other hand it also makes them very surface sensitive, which is an advantage when doing surface science.

A more exotic probe for materials and surface science is the x-ray. X-rays are photons (and/or electromagnetic radiation) in the 100 eV - 100 keV energy range (visible light is in the 2 - 3 eV range). The energy of the photon is given by $E = \frac{hc}{\lambda}$, where h is Planck's constant, c is the speed of light in vacuum and λ is the wavelength. X-rays in the lower range (up to about 1 keV, "soft x-rays") are often used for photo electron spectroscopy[1], as many atomic core levels are in this range. X-rays in the higher range ("hard x-rays", > 6 keV) are used for x-ray diffraction and absorption. This is because x-rays below about 6 keV have too long wavelengths for diffraction of atomic lattices, and the penetration depth through windows and gases is too small to be practical for those applications [1]. Typical energies for x-ray diffraction we have used are about 17 keV (0.73 Å) and upward. In the home lab x-rays are generated with sources based on the rotating anode technology: a metal anode is bombarded with an electron beam and x-rays are generated by the electrons being decelerated in the anode (*Bremsstrahlung*, charges under acceleration emit electromagnetic radiation), and by the emission of x-rays from fluorescence from the anode. The bremsstrahlung energy is continuous while the fluorescent x-rays have precisely defined energies. Lab sources are limited in the intensity of the x-ray beams they can produce as well as the energy resolution they can achieve (the energy of the fluorescent x-rays is also set). To generate higher quality x-ray beams, synchrotrons have been developed.

---

[1] Or photons in the high ultra-violet.

0.2 Synchrotrons

Synchrotrons generate x-rays based on the fact that electrically charged particles send out electromagnetic radiation when they are accelerated (similar to Bremsstrahlung). Through controlling a beam of electrons with great precision, x-rays beams of high intensity and with well defined and tunable energy can be generated. The intensity of the beam is important in experiments where the changes in the sample happen quickly and one wants to capture the dynamics. The quality of the beam (energy spread, coherence, collimation) is important for high precision x-ray diffraction (XRD) experiments. The tunable energy is necessary for the x-ray absorption spectroscopy (XAS) technique, and allows for varying the electron escape depth in other techniques like x-ray photo electron spectroscopy (XPS).

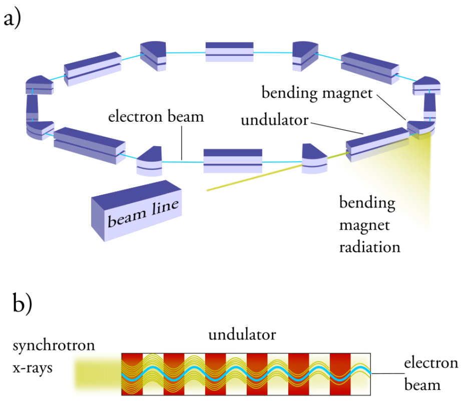

Figure 4.1: a) The layout of a synchrotron. b) The undulator.

Without going into too much detail, a few words can be said about how synchrotrons work. As already mentioned, they rely on the acceleration of electrons to generate x-rays. The electron beam is supplied by a linear accelerator based on radio frequency resonant cavities. In short, the electric field in the radio waves accelerate the electrons in the propagation direction of the waves, by the electrons "surfing" on the radio wave[2]. The electrons are accelerated to energies of a few GeV or more. They are then inserted into a storage ring that they travel around continuously. A sketch of the ring is shown in Figure 4.1 a). This ring shape brings the thoughts to the large hadron collider (LHC) at Cern, but its not a collider, the electrons are not supposed to collide with anything. The electrons are kept in the ring by magnets that bend their path along the direction of the ring (in this way the "ring" is really more of a polygon as the bending magnets sit in certain positions along the ring). In the bending magnets the electrons are accelerated toward the centre of the ring, and so they emit radiation. The energy of this radiation depends on the curvature of the beam path, making the energy tunable through the control of the strength of the magnetic field. This bending magnet radiation is used for the x-ray absorption (XAS) technique, as controlling the x-ray energy and intensity is very important for that technique. For most other applications the x-rays are generated using insertion devices such as undulators. They are situated along the straight sections of the "ring", and are much more efficient in generating x-rays than bending magnets. An undulator is an array of magnets with the field pointing alternately upward and downward. A

---

[2] The explanation is fanciful, but accurate.

sketch is shown in Figure 4.1 b). It has two blocks of magnet arrays and the electron beam travels in between the blocks. As the field periodically changes direction the electrons are oscillated from side to side along the undulator[3]. The acceleration generates x-ray radiation, and if the periodicity of the magnet array is right, the radiation generated in all the segments will be in phase. This results in a high intensity x-ray beam with contributions form every segment of the undulator. The energy will also be well defined as the energy depends on the harmonic frequencies of the undulator. The field strength at the electron beam path can be changed by altering the gap between the blocks making up the undularor.

The x-ray beam exits the undulator and enters one of the experimental stations at the synchrotron, called a beam line. There the energy resolution further improved, the beam is focused, directed and split up in several depending on the application. One of the most important components is the monochromator, which selects one single energy from the beam. The monochromator is a set of diffraction gratings, usually made from two silicon blocks[4]. The beam is focused and directed at the beam line using mirrors based on silicon. The beam lines we have used the most during by work is the HIPPIE beam line [119] for x-ray absorption spectroscopy (XPS) and the BALDER beam line [24] for x-ray absorption spectroscopy (XAS) at the MAX IV synchrotron outside Lund.

0.3 The photoelectric effect

The photoelectric effect was discovered by Hertz in 1887 and explained later by Einstein in 1905[5][56]. It is the core phenomenon to understand and explain both XPS and XAS, so it will be explained here first before the experimental techniques are presented. In essence, the photo electric effect is when a photon encounters an electron bound in a material system (like a solid, liquid, molecule or atom) and transfers all of its energy to that electron, causing it to escape the system into the surrounding space. This causes an electrical current of sorts, hence the name. In order to liberate the electron, the energy of the photon needs to be higher than the energy binding the electron to the system, otherwise no absorption can take place. A schematic picture of the photoelectric effect is shown in Figure 4.2. What happens with the electron when it has been emitted depends on what is around the absorbing atom, and will be discussed later. In the following paragraphs some fundamental theoretical considerations will be discussed.

The first thing to consider when discussing the photoelectric effect is the absorption of the photon by an electron in the system. In the following description the atom before the absorption event is called the initial state, and the ionized atom and emitted electron after

---

[3] In principle, it operates like an x-ray antenna.

[4] the grating consists of the crystal planes in the silicon: for the short wavelengths of the x-rays one needs a fine grating.

[5] for which he was awarded a Nobel prize

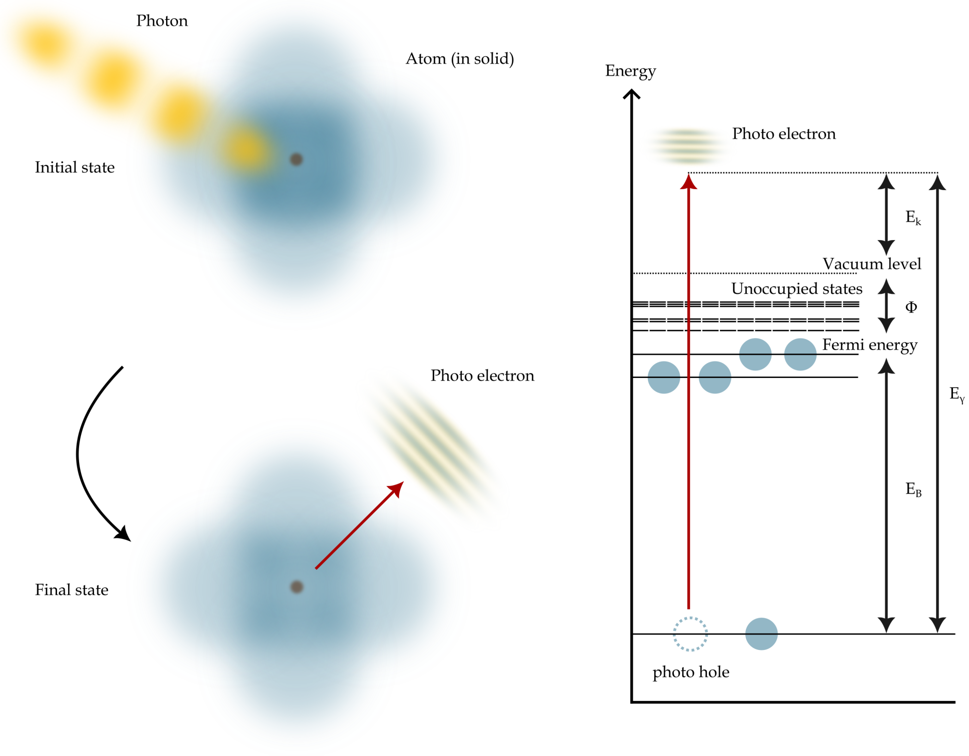
Photon
Atom (in solid)
Initial state
Photo electron
Final state
Energy
Photo electron
E_k
Vacuum level
Unoccupied states
Φ
Fermi energy
E_γ
E_B
photo hole

Figure 4.2: The photoelectric effect. An electron in an atom (in a solid in this case) absorbs all the energy of an impinging photon, emitting the electron into space. The difference between the photon energy and the energy binding the electron to the system becomes the kinetic energy of the photo electron.

absorption is called the final state. The absorption is a statistical process governed by the quantum mechanics of the system. The number of transitions from initial to final states per second (W) can be described by Fermi's Golden Rule, which is formulated as [1]:

$$W = \frac{2\pi}{\hbar} |\langle\psi_f|\mathcal{H}_\mathcal{I}|\psi_i\rangle|^2 \rho\left(E_f\right) \tag{4.1}$$

where π and $\hbar$ are constants, ψ_f the wavefunction of the final state, ψ_i the wavefunction of the initial state, $\mathcal{H}_\mathcal{I}$ is the interaction Hamiltonian and $\rho(E_f)$ is the density of states around the Fermi energy E_f. For photo absorption, the transition probability will be proportional to $W \propto |\langle\psi_f|\mathcal{H}_\mathcal{I}|\psi_i\rangle|^2\delta\left(E_f - (E_i + E_\gamma)\right)$, where the delta function states that the energy must be conserved (the energy of the final state (E_f) must be equal to the energy of the initial state (E_i) plus the energy of the photon (E_γ)) [56]. A key fact that follows from Fermi's Golden Rule is that the probability is proportional to the overlap between the wave functions of the initial and final states. That is, the more similar the excited, ionized atom plus photo electron (ψ_f) is to the atom before absorption (ψ_i), the more likely the electron is to absorb the photon. Calculating the wave functions is difficult, as they are complicated many body systems where the electrons all affect each other (atomic physicists spend considerable time and effort understanding the energy levels in atoms). This is especially true for the final state, where the missing photo electron causes all the other electrons in the atom to adjust their energy according to the new charge distribution they are experiencing (called relaxation). The resulting ion may also have several excited states it can go into during photo absorption. Obtaining a quantitative theoretical understanding for the photo absorption process is therefore very difficult. For a conceptual understanding of the experimental techniques it is enough to remember that the absorption process is proportional to the similarity between the initial and final states, that a multiple of possible final states exist, and that the energy needs to be conserved.

The conservation of energy is a law of nature, but there is a principle that must be considered when dealing with energy conservation during photo absorption. It is Heisenberg's uncertainty principle, which states that[74]:

$$\Delta E \Delta t \geq \frac{1}{2}\hbar \tag{4.2}$$

where ΔE is the uncertainty in energy, Δt the uncertainty in time and $\hbar$ is the constant $1.055 \cdot 10^{-34}$ Js (Planck's constant divided by 2π). The significance is that energy and time cannot be simultaneously determined, some uncertainty must remain in at least one variable. This means that if something exists for a very short time (meaning that the certainty in time is high), the energy is inherently uncertain (and vice versa: if the energy of something is very certain, such as the total energy of the world, its lifetime is very uncertain). This does not affect our macroscopic world, as $1.055 \cdot 10^{-34}$ Js is a very small number, but in units more natural for atoms it is $\frac{1}{2}\hbar \approx 0.3$ eV fs. This means that something that exists for about a femtosecond, the uncertainty in energy is about 0.3 eV. If an electron in an atom absorbs a photon and is emitted it leaves behind a hole in the atom, which will eventually be filled by another electron in the system. How quick this process is will determine the hole lifetime, and through the Heisenberg principle the certainty in the energy associated with creating the hole in the first place. If the photo hole lifetime is short, it can form with an energy noticeably larger or smaller than what is dictated by the conservation of energy. This variability of the energy will eventually show up in the kinetic energy of the photo electrons, and in the data generated from them.

There are two main routes along which the core hole in the atom may be filled. In both cases an electron with a lower binding energy decays to fill the hole and releases the excess energy. The energy can be released as an x-ray photon with the energy equal to the difference in energy between the levels the electron passed between. These x-rays are called fluorescent x-rays or characteristic x-rays. Because the electron can come from several higher shells there will be several x-rays of similar energy for each core level. The energy of the x-rays will be very well defined, and can be used to identify which atom emitted the x-ray (hence the name characteristic x-rays). This is used as a technique in itself, and the fluorescent x-ray emission can also be used when doing x-ray absorption spectroscopy. The energy released when the electron fills the core hole can also be transmitted to a second electron in the atom, emitting it from the atom. This second route of filling the core hole is called Auger emission and the emitted electron an Auger electron[6]. For the same reason as in x-ray fluorescence, the Auger electrons can have different energies, but are all characteristic of the atom that emitted them. The Auger emission is also used as a technique for characterising materials, and will be described briefly in a later part of this thesis. The Auger electrons can also be detected during X-ray Photoelectron Spectroscopy, potentially causing confusion.

1 Spectroscopy

Spectroscopy as a method uses how matter interact with radiation or particles of some type as a function of the energy of the radiation or particle. Originally, only electromagnetic radiation (photons) was used for spectroscopy, but now other types of probes are used as well, such as electrons, ions, etc. Typically, spectroscopy provides averaged information of the sample, where all parts of the sample illuminated by the radiation contributes to the spectrum[7]. The most common type of information to get from spectroscopic techniques is elemental and chemical information.

1.1 X-ray Photoelectron Spectroscopy (XPS)

X-ray Photoelectron Spectroscopy (XPS) is an experimental technique based on the photoelectric effect, described earlier. The energy of the emitted electron (as well as its angle of emission and other properties) depends on the environment in the material it escaped, and thus information about the material can be obtained by studying the emitted electron. The general name of the technique to study materials, molecules and atoms in this way is Photo Emission Spectroscopy (PES), and its use for chemical analysis was invented and developed by Siegbahn[101] (and then it is also sometimes referred to as ESCA (Electron Spectroscopy for Chemical Analysis)). Photons of any energy sufficient to cause photo emission from the sample can be used for PES, from ultra violet and upward, but photons in the x-ray energy range have been found perhaps the most useful for studying material properties. Many electrons in a material are core electrons with binding energies in the range of a few hundred eV or more, and photons with energies in the x-ray range are required for emitting them from the atoms they are bound to. For studying the chemical composition of materials, one is typically interested in the difference in energy of the photo electrons from atoms in different chemical environments. By comparing these energies with each other and with measured references it is possible to determine the chemical composition and answer the scientific question posed. Next, let us consider the energy of the emitted electron.

---

[6] Named after Pierre Victor Auger who discovered them in 1923.

[7] although some set-ups are designed to do spectroscopy, microscopy or diffraction simultaneously.

If the photo electron is emitted from a solid, the energy of the electron is given by[1]:

$$E_{kin} = E_\gamma - \left(E_f - E_i\right) = E_\gamma - E_B - \phi \tag{4.3}$$

where E_γ is the photon energy, E_f is the energy of the final state, E_i the energy of the initial state, E_B is the binding energy of the electron and ϕ is the work function. The energy threshold the electron needs to overcome to free itself from the solid is called the vacuum level: the energy of an electron in vacuum. Knowing the energy of the final state requires knowing the state of the ionized, excited atom and the emitted electron (ψ_f), which is very difficult. Fortunately, we do not need to know it to use the XPS technique. The practical way to obtain useful spectra is to measure reference compounds of certain, known, compositions and compare the binding energies found for the references with those from the experimental data. The binding energy is defined as the difference in energy between the bound electron and the highest occupied state in the system, at the Fermi energy E_F. In a metal the Fermi energy would be that of the electrons in the conduction band with the highest energies. However, also an electron at the highest occupied state needs some additional energy to escape the solid and become truly free, and this energy is described by the work function ϕ (the work function is affected by, for example, the coverage of molecules adsorbed on the surface, and so it can be used to extract information about the chemical environment of a surface). As the work function depends on the material as well as on the conditions the material is in, it makes the kinetic energy of the photoelectron an unreliable property for material characterisation. Relative to the vacuum level, the energy of the bound electron and the Fermi energy are equally affected by changes in the work function. By defining the binding energy as the difference between energy of the bound electron and the Fermi energy, one avoids work function changes affecting the measured binding energies. With these definitions, let us move on to how an XPS spectrum looks like and why.

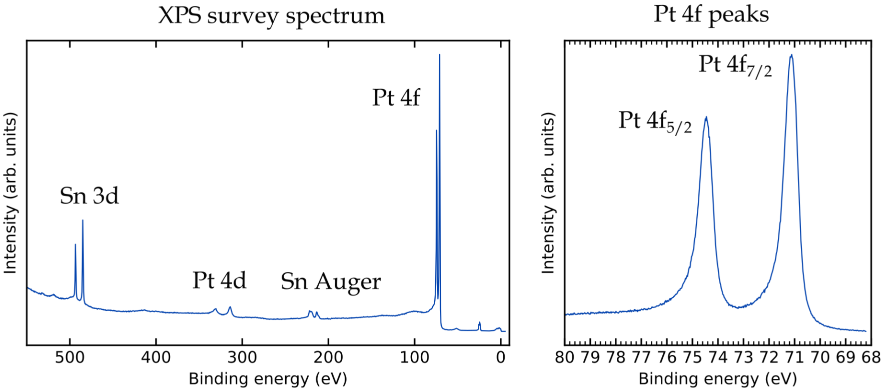

Figure 4.3: A survey XPS spectrum of a Pt(111) single crystal with Sn on (left) and a close up of the Pt 4f peaks (right). The spectrum was recorded with a photon energy of 650 eV.

In Figure 4.3, an XPS spectrum of a Pt(111) surface with a Pt_3Sn surface alloy on top is shown, as well as the Pt 4f peaks in closer detail. The peaks that are seen are from electrons from the different electronic shells of the elements that are on the surface. All peaks are from filled core shells, valence electrons would show up as a band at binding energies near the Fermi energy. The most prominent peaks are the Pt 4f peaks, as this shell has the most electrons of those that are in the spectrum (f means that J = 3, leading to $J(J+1) = 12$) and that Pt is the most abundant element in the Pt single crystal sample. The more tightly bound Pt 4d peaks are also visible, as are the Sn 3d peaks from the deposited Sn. There are two peaks at around 430 eV as well, and they are Auger peaks from Sn. Auger emission is when an electron is emitted from an atom as a result of a core hole being filled (one less tightly bound electron fills the core hole and another electron somewhere in the atom is emitted with the energy released in the decay process). For Sn these electrons are emitted with a fixed kinetic energy of about 430 eV independent of the photon energy. Auger peaks are used for surface analysis as well as photoemission peaks, and the technique will be presented later.

When doing XPS analysis, one typically examines the peaks and the shape of the peaks in closer detail than in the survey spectrum. The Pt 4f peaks in figure 4.3 (right) is an example. First, we note that there are two peaks. This is caused by spin-orbit splitting, which is that the emitted electron can couple parallel or anti parallel to the angular momentum of the atom. The angular momentum of the atom is 3 (f: J = 3), and the spin $\frac{1}{2}$ electron then couples to yield a total angular momentum of 2.5 (or 5/2) or 3.5 (or 7/2). We also note that the intensity is higher in the background in the left hand side of the spectrum (higher binding energy) than on the right (lower binding energy). This is due to some electrons scattering and losing energy, making them appear more tightly bound to the detector. This background is something that has to be considered when fitting XPS spectra.

The most common way to treat the background is with the Shirley algorithm [56], which ads a certain number to the background based on what the intensity of the spectrum is, going from low to high binding energy. For every electron emitted, there is a certain probability that it will scatter and go to the background. This is useful for peaks from elements that exist in the bulk, but in many cases, such as surface or minority species, it is often enough to assume a linear background.

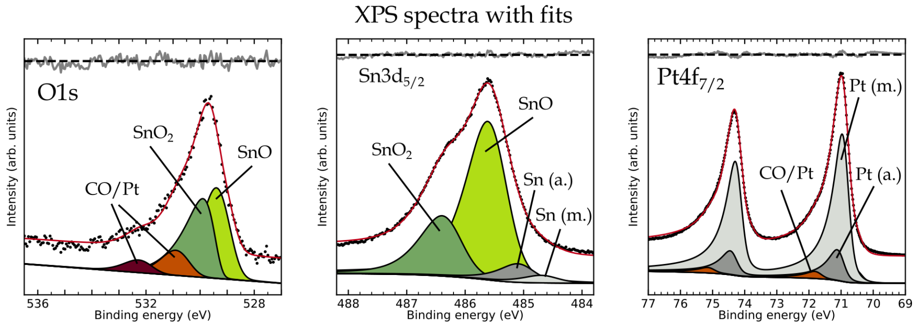

Figure 4.4: XPS spectra of an oxidized Sn/Pt(111) surface.

The shape of the peak itself is also affected by the physical processes involved in the photoemission process and the detection of the photo electron. We have seen that the Heisenberg uncertainty principle make the energy uncertain if the lifetime of the core hole is short. This is something that causes the kinetic energy of the photo electrons to vary, and broadens the peak shape. This broadening has a Lorentzian distribution. There are many other factors that cause broadening, for example that electrons may collide during their journey through the analyzer, random inhomogenities in the atomic environments etc. which have a random distribution. Random variations result in a Gaussian distribution, and thus the peak shape will be a combination of Lorentzian and Gaussian. This peak shape is described by a convolution between a Lorentzian and Gaussian and is called a Voigt profile. Convolutions are computationally heavy, and often it is enough to use a pseudo-Voigt peak shape, which is a linear combination of a Gaussian and Lorentzian [97]. This is the shape I have used most often when doing peak fitting.

The binding energies of the core electrons are affected by which bonds the valence electrons participate in. The shift this causes in the core level peaks is called chemical shift, and is a big part of the reason why XPS such a useful technique. Atoms with different oxidation states can be distinguished, as well as more subtle differences such as being in the bulk or in the surface layer. In molecules, atoms in different positions can often be told apart by their shifts. In this way the chemical composition of the sample irradiated by the beam is obtained. XPS is an averaging technique, so one only obtains the average composition and nothing about the morphology or the species detected. If one detects both oxide and metal, for example, one cannot know if they are evenly spread over the sample or if they are separated into clusters. Such information has to be obtained by other means. Each chemical species can be represented by a peak of appropriate shape (for example the Voigt peak), and analysis of the spectra is typically done by assigning each peak that can be detected in the spectra to a chemical species. In some cases different species have very similar shifts, in which case peak assignment has to be done based on context or conditions. If spectral features contain several peaks closely spaced together one sometimes have to represent them with a single peak, which may have to have some degree of asymmetry.

As already mentioned, electrons are charged particles that interact strongly with matter. This has consequences for what can be measured with the XPS technique. As we have already seen, many electrons originating from the sub surface of the sample lose energy as they pass through the material to reach the surface and contribute only to the background. This means that the electrons in the measured peaks come mostly from a thin layer near the surface. How thin is this layer? This depends mostly on the kinetic energy of the photo electrons, and is for typical energies 3-30 Å, as can be seen in Figure 4.5. This means that the electrons come from the very topmost atomic layers (typical distances between atomic layers is around 3 Å for metals). For having a maximal surface sensitivity, kinetic energies around 100 eV are desired. The short mean free path of electrons in matter makes XPS very useful for measuring surface processes, for example surface chemistry and catalysis. This strength is also a weakness.

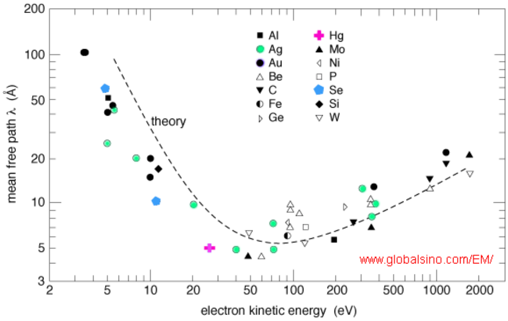

Figure 4.5: Electron escape depth. From ref [71].

Seeing how short the electron mean free path is, we can understand why (standard) XPS needs to be carried out in ultra high vacuum conditions. The range of the photo electrons in gas is longer than in a solid, but still very short compared to the sizes of the sample and the instrument. This brings us to the technical aspects of XPS. How, exactly, do you measure the kinetic energy of the photoelectron?

Experimental setup for XPS

To make use of the photo electrons for extracting information about the material system, we need a machine to measure their kinetic energy. Depending on the experiment, the kinetic energy may range in the order of a few eV to a few keV. One electron volt (eV) is 1.6×10^{-19} Joules, and it is necessary to measure the kinetic energy of each electron. The way this is done is by subjecting all the photo electrons by an electric field, bending their trajectories. The force acting on the electrons is determined by the field, and is independent on the kinetic energies of the photo electrons. Photo electrons with lower kinetic energies (slower) will have more bent trajectories than those high higher kinetic energies. They will then end up in slightly different parts of the instrument, and so the kinetic energy can be determined by observing where the photo electrons hit the detector. In essence this is how X-ray Photoelectron Spectroscopy is done.

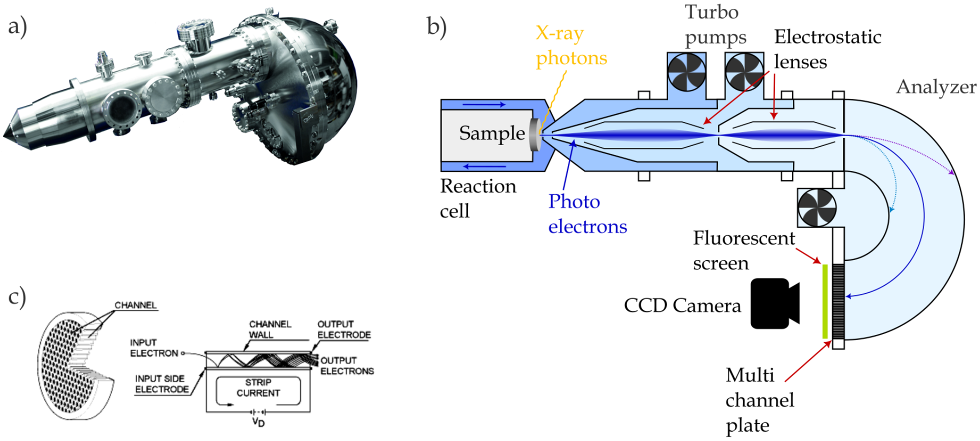
a)
b)
X-ray photons
Turbo pumps
Electrostatic lenses
Analyzer
Sample
Reaction cell
Photo electrons
Fluorescent screen
CCD Camera
Multi channel plate
c)
CHANNEL
INPUT ELECTRON
INPUT SIDE ELECTRODE
CHANNEL WALL
OUTPUT ELECTRODE
OUTPUT ELECTRONS
STRIP CURRENT
V_D

Figure 4.6: a) a photo of an electron analyzer (Scienta). b) a model of the analyzer in a), with the pumping stages indicated, and c) a model of the multi channel plate that detects the photo electrons (from DM electronics).

The field bending the trajectories of the photo electrons comes from a hemispherical shell, which is easily identified on the instrument. A photograph of an electron analyzer is shown in figure 4.6 a). In the analyzer, a number of lens elements are also needed to control the electrons. To detect the electrons, a multi channel plate (MCP) is typically used. A single electron has a very small charge (1.6×10^{-19}C) and the signal benefits from being amplified. When an electron enters one of the channels in the MCP and hit the chamber wall, it releases a number of electrons, which are accelerated by a high voltage in the channel. The newly released electrons will repeat the process in an avalanche-like process (Figure 4.6 c). In this way even a single electron will trigger an appreciable current to be detected. Typically, the electrons are then made to strike a fluorescent screen to create light[8], which is then detected by a camera.

---

[8] much like in an old-fashioned cathode ray TV screen.

Near Ambient Pressure XPS (NAP-XPS)

We have seen how XPS is a useful technique to study the chemistry of materials, but that the electrons require ultra high vacuum to travel from the sample and through the instrument in order to be detected. However, many scientific questions in our field revolve around how surfaces interact with gases at or above atmospheric pressures (or in liquids). The Near Ambient Pressure X-ray Photoelectron Spectroscopy technique (NAP-XPS) was developed to be able to measure on samples in more realistic conditions. Briefly, the idea of the technique is to allow higher pressures just above the sample surface, while still keeping the pressure low in the electron analyzer. If the high pressure region is thin, enough electrons can pass through it and reach the analyzer where they can travel more freely and reach the detector. It requires the addition of some components to the electron analyzer unit. In figure 4.6 b) the pumping stages of an electron analyzer are illustrated. The insides of the analyzer consists of several compartments that are pumped separately and only connected by narrow apertures (to allow the photo electrons to pass). This differential pumping is done to efficiently lower the pressure in the analyzer. In this way the pressure can be a few mbar at the sample and about 10^{-8} mbar in the analyzer. Standard NAP-XPS allows studying samples at pressures around 1-10 mbar, which is orders of magnitudes higher than without the differential pumping and enough to follow the dynamics of chemical reactions. However, it is still a thousand times lower than atmospheric pressure. There is one /are a few XPS set-ups that can measure at atmospheric pressures by pushing the design to the limit [29].

1.2 X-ray Absorption Spectroscopy (XAS)

The X-ray Absorption Spectroscopy technique is based on the photoelectric effect just like XPS, but instead of measuring the photo electron directly one measures the number of photons absorbed by the sample. The intensity drop as the x-ray beam travels through the material is described by Beer's law [79]:

$$I = I_0 e^{-\mu x} \tag{4.4}$$

where I is the intensity of the beam in the sample, I_0 is the intensity before entering the sample, μ is the absorption coefficient, and x is the distance travelled. The equation basically states that for every unit of distance the beam travels through the material, x-rays have a certain probability of being absorbed, which is described by μ. The absorption coefficient itself is a function, described by $\mu \approx \frac{\rho Z^4}{AE^3}$ where ρ is the sample density, Z is the atomic number, A is the atomic mass and E is the x-ray energy. We see that heavier elements will have much higher absorption (Z^4) than lighter ones and that the absorption decreases with x-ray energy ($\frac{1}{E^3}$). For many applications, such as medical imaging, this is enough information. In order to have photo absorption the energy of the photon needs to be sufficient to liberate an electron from the atom. This leads to a strong, element and shell specific contrast when the x-ray energy is close to the binding energy of an electron in the sample: there will be no absorption at photon energies just below the binding energy of the electron and strong absorption just above. This introduces a step-like feature in the absorption probability as a function of energy near the binding energy of an electron in the material. The probability of absorption is also affected by the behavior of the photoelectron in the material after the absorption event, and this provides a wealth of information about the material system. In order to describe these phenomena well, the so-called fine structure function is defined as $\chi = \frac{\mu(E)-\mu_0(E)}{\Delta\mu_0(E)}$, where $\mu(E)$ is the absorption coefficient of the material, $\mu_0(E)$ is the absorption coefficient of a single atom (which lacks fine structure), and $\Delta\mu_0$ is the edge jump at the threshold energy of the electron in question. In this way the fine structure is separated out from the other parameters affecting the absorption probability. The fine structure phenomenon will be described in the following paragraphs. From a practical perspective, measuring the photons instead of the photo electrons has benefits as well as drawbacks. Most importantly, x-rays can penetrate matter much more easily than electrons, and so one is less limited by the presence of gases or liquids above the sample than in XPS. This also means that the measured signal can originate from much deeper in the sample than in XPS. For measuring surfaces and the processes occurring on them it introduces new challenges. Before discussing these practical aspects further, a brief theoretical description of x-ray absorption will be given.

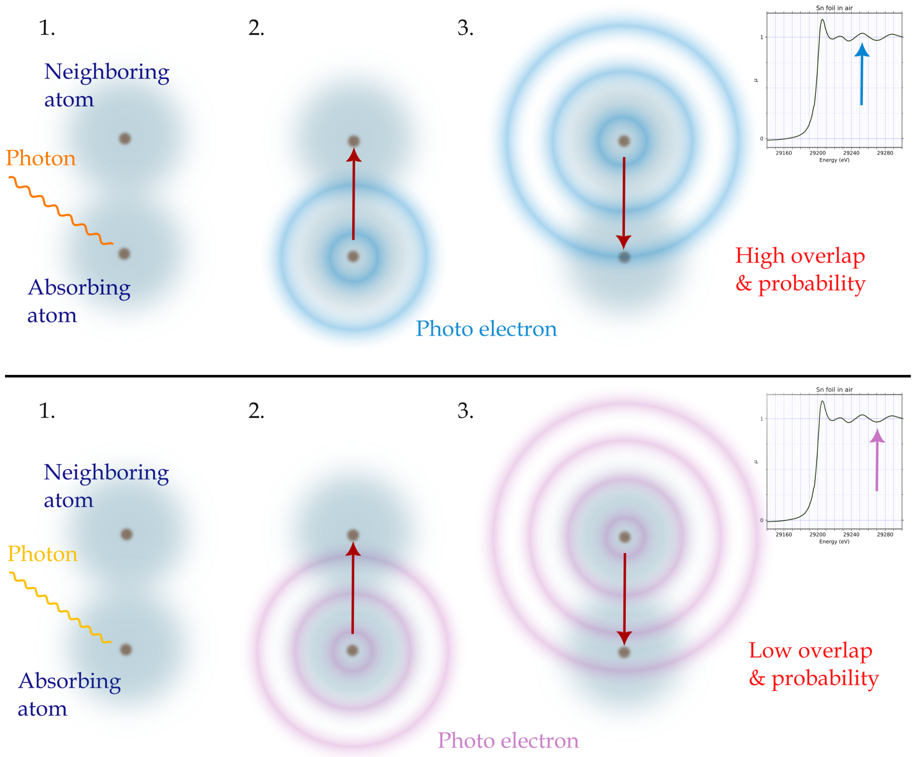
1.
2.
3.
Neighboring atom
Photon
Absorbing atom
Photo electron
High overlap & probability
Sn foil in air
1
0
29160
29200
29240
29280
Energy (eV)
1.
2.
3.
Neighboring atom
Photon
Absorbing atom
Photo electron
Low overlap & probability
Sn foil in air
1
0
29160
29200
29240
29280
Energy (eV)

Figure 4.7: An illustration of the principle behind X-ray Absorption Fine Structure (XAFS). 1. The photo absorption process, 2. The photo electron being emitted from the absorbing atom, 3. The photo electron scattering of a neighbouring atom toward the absorbing atom. In the top panel the photon energy is slightly lower than in the bottom panel.

To understand what information can be obtained from the fine structure of XAS, let us briefly revisit Fermi's Golden Rule (Equation 4.1). It states that the probability of a quantum mechanical event, such as photo absorption, to occur is higher the greater the overlap of the initial and final wave functions of the system. In simple terms, if the electrons in the atom after absorption have positions similar to those of the atom before absorption, absorption is more likely. The electrons that stay in the atoms may change slightly after photo emission, but not very much. They do not affect the probability of photo emission very much. However, the photo electron is ejected from the atom by the photo emission process and how it travels in the material has a strong effect on the overlap of the initial and final wave functions, and therefore also the probability of absorption. This is counter intuitive for a mind not familiar with quantum mechanics: whether the electron will be absorbed or not depends on what it will do in the future. But we have to accept it. The greatest wave function overlap is achieved if the ejected photo electron returns to the atom it came from, which can happen if the electron scatters from neighboring atoms. The photo electron must be treated as a wave, meaning that the amplitude oscillates along the path it takes. The frequency of this oscillation depends on the wavelength (and therefore energy) of the photo electron. This introduces an energy dependence of the probability of photo emission: even if the photo electron would return to to the atom it came from, if the amplitude of the photo electron wave function is low where the atom is, the probability of photo emission would be low. Conversely, if the amplitude is high where the atom is, the probability of photo emission is high. This can be illustrated as in Figure 4.7: for a certain path the photo electron takes, the amplitude at the absorbing atom will alternate between high and low values depending on the wavelength (and therefore energy) of the photo electron. The probability of absorption related to the fine structure effects as a function of energy of the photoelectron can be described by the daunting-looking equation:[20]

$$\chi(k) = S_0^2 \sum_i N_i \frac{f_i(k)}{kD_i^2} e^{-\frac{2D_i}{\lambda(k)}} e^{-2k^2\sigma_i^2} \sin\left(2kD_i + \delta_i(k)\right) \tag{4.5}$$

where k is the wave vector of the photo electron and is related to the wavelength (λ) as $k = \frac{2\pi}{\lambda}$, and energy as $k = \frac{1}{\hbar}(\sqrt{2m_e(E - E_0)})$, where m_e is the mass of the electron, E is the energy of the photon, and E_0 is the energy required to liberate the electron. The core of the equation and the XAFS phenomenon is the last part of Equation 4.5: $\sin\left(2kD_i + \delta_i(k)\right)$, where D_i is the distance the photo electron travelled before it returned to the absorbing atom and δ_i is a phase shift introduced as the electron scatters from atoms in the material. The sinusoidal dependence on k is the result of the oscillation in the photo electron wave function amplitude at the absorbing atom discussed previously and illustrated in Figure 4.7. The sum over the index i is to account for all different paths that the photo electron can take. The other factors account for various effects and phenomena that modulate the probability. S_0 is an element specific constant that takes into account that the overlap between the absorbing atom and remnant ion is not perfect (see Fermi's golden rule), N_i is a degeneracy term, taking into account that there are several paths of the same length, f_i is the probability of the photo electron to scatter elastically when encountering an atom, the kD_i in the denominator is to account for that the probability density of the (spherical) photo electron wave function gets lower with distance from the absorbing atom, $e^{-\frac{2D_i}{\lambda(k)}}$ accounts for that the ionized absorbing atom will eventually decay (which changes its wave function and thus the overlap), $e^{-2k^2\sigma_i^2}$ accounts for disorder in the material (which affects the path lengths). Without going into too much theoretical detail, let us see how an x-ray absorption spectrum looks like and what it means.

There are different parts of an XAS spectrum, which are treated differently. The first part going from low to high energy is the edge region itself. Absorption starts taking place when the core electron gets enough energy from the x-ray to be excited to an available empty state. The lowest available states are abound states of the atom, that is, above the Fermi energy but below the ”vacuum level” where the electron becomes free (see Figure 4.2). The first thing to note about the edge energy is that the chemical shift effect discussed in the XPS chapter

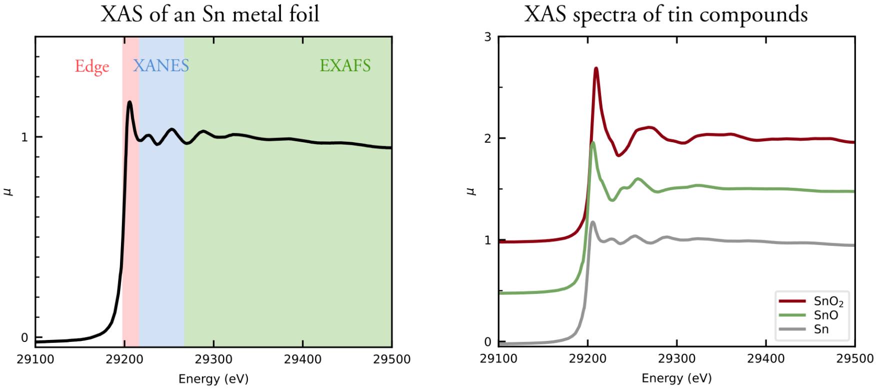

Figure 4.8: XAS spectra of some samples containing tin. Left: an illustration of what the different parts of the spectrum is called. Right: examples of spectra from a metallic tin foil, stannous oxide (SnO) and stannic oxide (SnO_2). These spectra are normalised to the edge jump.

(that *e.g.* the oxidation state of the atom affects the binding energies of the core electrons) affects also the XAS spectrum. For example, the spectrum from SnO_2 (with Sn^{4+}) has an edge that is slightly higher than SnO (Sn^{2+}) and Sn (Sn^0) in Figure 4.8. XAS spectra are usually normalised to the size of the edge jump, as in Figure 4.8. After the edge, a high peak is seen, it is called the ”white line” for historical reasons. Understanding why the edge region looks like it does is easier to imagine from an intuitive perspective than to calculate it exactly. One needs to do an atomic physics calculation and find all the energy levels of the atom, which is very cumbersome. Fortunately, we do not need to do this to use the XAFS technique, and the phenomena get simpler the higher energy the photo electron has.

At a few eV above the edge, the electron gets enough energy to escape the atom and into the surrounding region. When the photo electron has low kinetic energy of a few dozen eV, it typically scatters multiple times before returning to the atom [1]. This region is called the X-ray Absorption Near Edge Structure (XANES), and is still relatively complex due to the multiple scattering of the photo electron. The spectrum in this region can be calculated using Green's functions (which is a clever way of solving differential equations), which is described in grater detail in Refs. [89, 90]. I will not go into greater detail how these calculations are done here. A common way to analyze XAS spectra in the XANES region experimentally is to compare experimental data to measured reference compounds. If the sample contains a mixture of the material references, its composition can be modelled as a linear combination of the references (called Linear Combination Analysis, LCA). For LCA to work, the signal to noise ratio of the data needs to be high enough, as relevant reference compounds often share many similarities. Telling them apart requires precision. A problem with LCA may arise if the sample contains a material or a phase for which there is no reference available. In this case calculations may be an option, for example with the Green's function approach mentioned earlier. LCA uses the entire reference spectrum as a comparison to the data. Another approach is to compare only parts of the experimental spectrum to the reference compounds, which is useful when there is a part of the spectral range that clearly differentiates the references with the rest of the range being ambiguous. The features need not represent anything physically meaningful, as long as they are useful for differentiating the spectra. This paragraph has dealt with analyzing the XANES region, where the (multiple) scattering of the photo electron is complicated. At higher kinetic energies, other tools become available for understanding the x-ray absorption spectra.

When the photo electron has a kinetic energy of above about 50 eV multiple scattering events become rarer and the absorption probabilities become easier to model using the XAFS equation (Equation 4.5). The analysis of the spectra in this region is called Extended XAFS (EXAFS). I have not used it in my work, but in essence one makes a Fourier transform of the spectrum as a function of k to obtain the scattering path lengths in the sine part of equation 4.5. With the path lengths together with the phase shift δ one can obtain how many neighbours the absorbing atom has, which elements they are and how far they are from the absorber. It is a powerful technique, Refs. [20, 79] are useful sources for information on EXAFS.

Experimental setup for XAS

In order to measure the absorption due to the fine structure effects of a sample, one needs an x-ray source with variable photon energy. For this reason XAFS is (with a few exceptions) a synchrotron technique. To obtain the absorption coefficient, one needs to measure the beam intensity before and after the sample (I and I_0 of Beer's law, Equation 4.4) to obtain μ as $\mu = \log\left(\frac{I}{I_0}\right)$. The absolute intensity of the beam can vary depending on the x-ray source and the optics it passes through on its way to the sample. As knowing the energy of the x-rays is very important and setups can vary slightly from beam line to beam line, one typically also measure a reference compound to which to calibrate the experiment spectrum. This reference is placed behind the second ion chamber and is measured with the same beam used to measure the sample. A sketch of the setup is shown in Figure 4.9. The beam intensities are measured with ion chamber detectors. This mode of measuring is called transmission mode, as it is the x-rays transmitted through the sample that are measured. This is the most straightforward way to measure and works well if the sample absorbs about half of the incident beam and this absorption is due to absorption by the element of interest. This is because one needs good measurements of both I and I_0. Problems may arise if the sample is too thick so that there will be no intensity (I) left to measure after the sample, or if the measured element is dilute in the sample so that little of the absorption will show fine structure effects. In cases where transmission mode does not work very well, one can instead measure the fluorescent x-rays coming from the sample. For the energies above about 2 keV, x-ray fluorescence is more likely than Auger emission [79].

Measuring the fluorescent x-rays instead of the absorbed intensity allows measuring samples that are too thick to transmit the beam, and can be useful when measuring on dilute samples as the signal to noise ratio is typically higher than measuring in transmission mode [20]. But it introduces new challenges. The fluorescent x-rays have energies (by their very nature) that have a high probability of absorption by the element that emitted them. Thus, if they encounter many atoms of the element that emitted them, they will be absorbed and will not reach the detector. This problem is called self-absorption and is prevalent if the density of the measured element is high and the sample is thick. The fluorescent x-rays are usually detected using semiconductor-based detectors. One example where an energy dispersive detector is necessary is a sample of a thin layer of tin on a platinum single crystal surface. The platinum crystal is too thick to transmit the x-ray beam, the amount of tin on the sample is small, and fluorescence from the platinum greatly contributes to the signal.

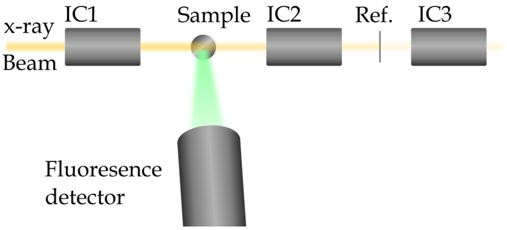

Figure 4.9: The setup of an XAS experiment. The beam passes through the three ion chambers (IC1-3), the sample and the reference. IC1 measures the initial beam intensity I_0 and IC2 measures the intensity after absorption I. IC3 measures the absorbed beam after the reference sample. The fluorescence from the sample can be used instead of IC2 to obtain I.

1.3 Auger Electron Spectroscopy (AES)

Auger electron spectroscopy (AES) is an electron-based technique that can be used to tell which elements are on a surface, and has some similarities to XPS. In fact, the Auger electrons show up when using XPS and analysing them can be useful, but in the home lab they are usually generated using electron beams rather than x-rays. A high energy (a few keV) electron beam is sent to the sample surface, where the electrons deposit their energy in the surface layer. This creates core holes in the atoms in the surface, and Auger electrons can be sent out as the core holes decay. These Auger electrons will have energies specific to the atomic transition of the decay, which means that Auger electrons from different elements can be told apart by their energy. In the home lab their energies are often measured using the same set-up used for LEED (shown in Figure 4.12, right). Compared to XPS, the energy resolution is lower, and core level shifts can be more difficult to distinguish with AES. The AES technique is mostly used for determining the quantitative elemental composition of the sample surface.

2 Diffraction

Diffraction uses the interference between waves to obtain information about the sample. Diffraction works the same way for any type of wave, be it a wave on the water, a sound wave, an electro magnetic wave (photon), or a particle (like the electron). Diffraction can tell something about the inter-atomic distances in a material, the atomic structure and also the shape of the scattering object. We use it mostly for finding the atomic structure. In order to use diffraction one wants to use a beam that is monochromatic (only one wavelength) and collimated. Diffraction works best with ordered structures. Increasing long-range order results in sharper and brighter diffraction spots.

For describing how diffraction works, let us consider an example. A beam of waves (for example electrons) is sent to the sample where the electrons scatter of the atoms, some of them elastically (without loosing energy). Diffraction is caused by the interference between waves that scatter from different parts of the sample, for example from different atoms. If the waves scatter at an angle, there will be a phase shift for the waves coming from different atoms relative each other. For most angles, the waves will be out of phase which strongly diminishes the beam intensity. Only when the waves are completely in phase will the intensity of the beam be preserved. The phase shift of the waves depends on the inter-atomic distances, so by measuring the angles where the waves are in phase one can calculate the inter-atomic distance (or the distance between scattering objects, which can be larger than atoms). An illustration of the principle behind diffraction is shown in the left part of Figure 4.10. In fact, diffraction can be used to measure any distance between objects that are more or less periodically spaced, not just single atoms. Multi-atom structures with long range order, like the tin surface oxides, can be detected well with diffraction.

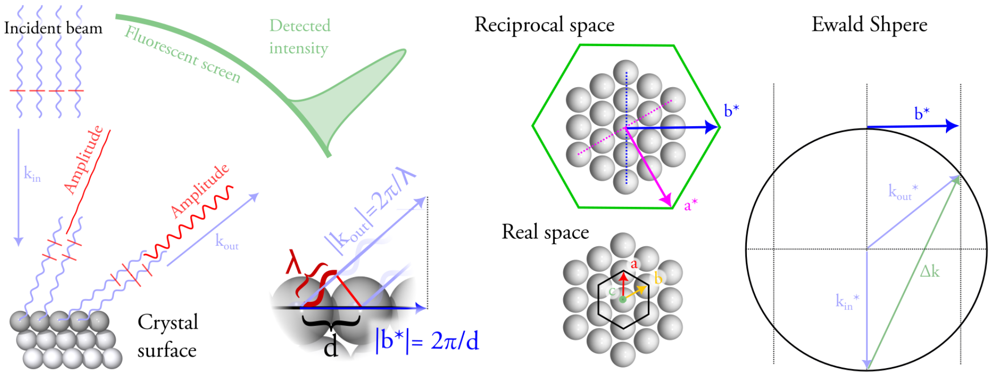

Figure 4.10: The working principles of diffraction. Left shows an example of when the scattered beam is out of phase (no intensity) and in phase (detected intensity). Middle shows the reciprocal space and the corresponding real space of a surface. Right shows the Ewald sphere.

More formally, the condition for diffraction maxima is determined by the reciprocal of the real space lattice vectors. If the real space vectors giving the position of the atoms on the surface are $\vec{a}$ and $\vec{b}$ (red and yellow arrows in the real space illustration in Figure 4.10), then the reciprocal vectors are defined as $\vec{a}^* = 2\pi\frac{\vec{b}\times\vec{c}}{\vec{a}\cdot\vec{b}\times\vec{c}}$ and $\vec{b}^* = 2\pi\frac{\vec{a}\times\vec{c}}{\vec{b}\cdot\vec{a}\times\vec{c}}$, respectively (magenta and blue arrows in Figure 4.10). $\vec{c}$ is a unit vector perpendicular to the surface. The result is that the direction of a reciprocal unit vector is perpendicular to the atomic planes (or lines in 2D), and the length is 2π divided by the inter-planar distance, d. The wave vector is $\vec{k} = \frac{2\pi}{\lambda}$, where λ is the wavelength. For a diffraction peak to occur, the difference between the incident and outgoing wave vector must be equal to a combination of the reciprocal lattice vectors: $\vec{k}_{out} - \vec{k}_{in} = \vec{G}_{hkl} = h\vec{a}^* + k\vec{b}^* + l\vec{c}^*$ where h, k, l are integers. For surfaces, the condition simplifies to $\vec{k}^{||}_{out} - \vec{k}^{||}_{in} = \vec{G}_{hk} = h\vec{a}^* + k\vec{b}^*$ if all scattering comes from the top layer ($\vec{k}^{||}$ denotes the component of $\vec{k}$ parallel to the surface). The Ewald sphere is used to visualise the diffraction condition: the radius is $2\pi/\lambda$, its position determined by the angles between $\vec{k}_{in}$ and $\vec{k}_{out}$, and if a reciprocal lattice vector lies on the sphere there will be a diffraction peak. in 2D the diffraction condition in the $\vec{c}$ direction becomes irrelevant and diffraction peaks go from spots in reciprocal space to lines (or rods). This is visualised as projections of the reciprocal space plane onto the Ewald sphere. For the example in Figure 4.10, the outgoing wave vector $\vec{k}_{out}$ is projected on the reciprocal lattice vector $\vec{b}^*$ and a diffraction peak is observed in the direction of $\vec{k}_{out}$.

2.1 Surface X-Ray Diffraction (SXRD)

X-ray diffraction can measure inter-atomic distance with very great precision. This is due to the possibility to create high quality x-ray beams with very well defined energy, and that the scattering angles can be measured very accurately. X-rays at the energies used for diffraction have relatively long range due to their low absorption in matter and the intensity of the diffracted beam is usually measured a few to several meters from the sample. It is a standard tool in materials science used to characterise samples and identify minerals, phases etc. When we use it to measure the structure of the single crystal surfaces, the technique is called surface x-ray diffraction (SXRD). X-rays do not interact very strongly with mat-

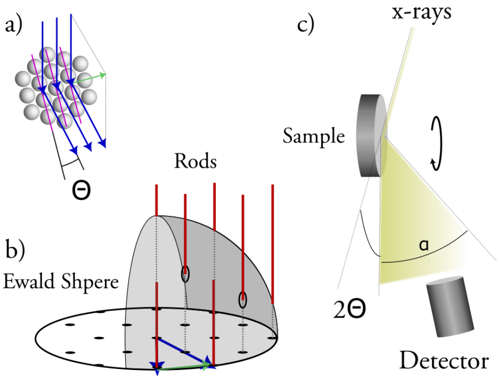

Figure 4.11: Surface x-ray diffraction. a) The diffraction condition in the plane. b) The Ewald sphere and rods from the surface structures intersecting it. Note that only some rods are plotted. c) The experimental set-up for Surface x-ray diffraction (SXRD).

ter (compared to electrons) and the penetration depth is long compared to the atomic layer spacing. This introduces challenges when measuring surfaces. To ensure that the x-rays scatter from the surface to a great an extent as possible, they are made to strike the surface at a very low angle. This geometry is called grazing incidence. If the angle is lower than the critical angle of the material, the x-rays will undergo total external reflection[9] and the field from the x-rays will only penetrate a few atomic layers down in the material. For this to work, the surface has to be very flat. By measuring the angle of the scattered beam in the plane of the surface (2Θ in Figure 4.11) one can obtain the structure of the surface as it appears in that plane.

One can also obtain information about how the surface structure looks like orthogonal to the plane of the surface. Examples include the number of layers of a some surface structure one has, the separation between the layers and the distance to the substrate etc. Because the diffraction comes from the very surface of the crystal one fulfils the diffraction condition along a line in reciprocal space rather than at a spot. These line are called rods, or crystal truncation rods, and they are shown in Figure 4.11 b). Intensity is seen where the rods intersect the Ewald sphere. The intensity of the rod is affected by the out-of-plane structure of the surface, so by measuring the intensity of the rod along its length one obtains structural information on the phase that caused that diffraction rod. This is done by moving the detector from near the plane of the surface to increasingly higher angles relative the surface plane (α in Figure 4.11 c). The intensity profile of the rods can be compared to theoretically calculated intensities to confirm the presence (or existence) of a proposed structure. For example, this was done in order to provide experimental proof of the calculated structure for the (4×4) $Sn_{11}O_{12}/Pt_3Sn(111)$ surface oxide in Ref. [75].

2.2 Reflection High Energy Electron Diffraction (RHEED)

RHEED stands for Reflection High Energy Electron Diffraction, and the setup is relatively simple. A high energy electron beam ($\sim$15 keV) is generated and shone on a sample at an angle almost parallel to the surface (grazing incidence, a few degrees), and subsequently reflecting from the surface. A relatively tightly spaced diffraction pattern (due to the short wavelength) is collected on a fluorescent screen on the other side of the sample. A sketch of the set-up is shown in Figure 4.12. Due to the beam coming from the side and the narrow angle of acceptance, only planes roughly parallel to the beam path can be detected for any one orientation of the sample: One sees a slice of reciprocal space at a time. To map out all of reciprocal space, the sample is rotated. The high energy of the electrons means the diffraction will not only be from the topmost layer and increase the amount of inelastic scattering (which only contributes to background), but it also makes it possible to operate at higher pressures than low energy electron techniques. The grazing incidence helps making the technique more surface sensitive and frees up space in front of the sample. This makes it possible to measure diffraction while treating the sample with gases or while depositing. This makes RHEED very useful for developing recipes for making samples, like the tin surface oxides featured in this thesis work, and it is mostly for this reason we have used it. For characterisation LEED is used more often.

---

[9] one can see total *internal* reflection by looking down the foot of a wine glass.

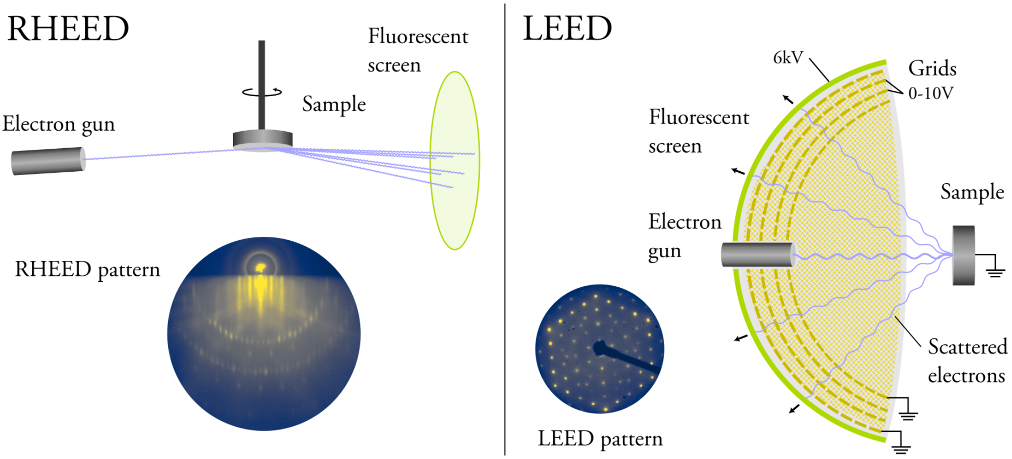

Figure 4.12: The RHEED setup (left) and the LEED setup (right).

2.3 Low Energy Electron Diffraction (LEED)

Low Energy Electron Diffraction works similar to the example shown in Figure 4.10: a low energy (typically 50-200 eV) electron beam is shone on the sample surface at 90° incidence, the back-scattered electrons are collected at a fluorescent screen where the diffraction pattern can be seen. The low energies make it very surface sensitive, and the signal comes from the top few layers. One sees all of reciprocal space at once, and moving further out in reciprocal space is easily done by increasing the beam energy. LEED set-ups are equipped with a few components to improve the signal. The first is a series of metal grids before the fluorescent screen. The two inner grids make it possible to filter out electrons that did not scatter elastically (background), while the grounded outer grids shield the rest of the apparatus from the electric fields. Due to the low energy of the electrons, they need be be accelerated to the screen (6 kV) to make enough of a signal to be detected. The set-up is shown in Figure 4.12. The pressures need to be low, and the apparatus needs to be in front of the sample. LEED was first used and reported in 1927 [27] and is now a very common surface science technique found in labs big and small, used for sample characterisation. A nice feature is that the LEED beam can be utilised in an electron microscopy technique called LEEM.

3 Microscopy

Microscopy techniques generate a real space image of the sample. For surface science, where we are concerned with the atomic-scale processes that happen on the surface, this is not trivial. Light microscopy has a resolution limit of about 200 nm, about one thousand times the size of an atom. To get atomic resolution or close to it, electrons or scanning probe techniques have to be used. There are no x-ray based techniques with atomic resolution yet. By far the most common electron microscopy techniques are scanning electron microscopy (SEM) and transmission electron microscopy (TEM), however, we have not used them in this work[10]. Instead we have used Low Energy Electron Microscopy (LEEM) (and X-ray Photo Emission Electron Microscopy (XPEEM) to some extent). We have also used scanning tunnelling microscopy (STM) and atomic force microscopy (AFM). These techniques will be explained in the following sections.

3.1 Low Energy Electron Microssopy (LEEM) & Photo Emission Electron Microscopy (PEEM)

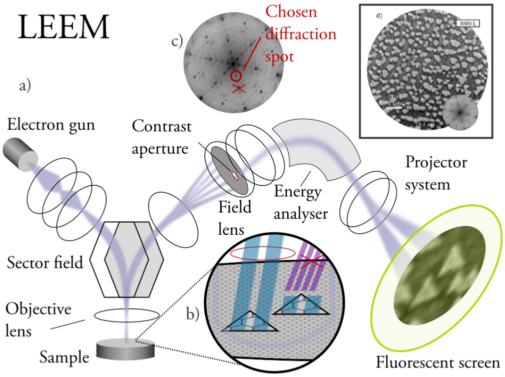

Figure 4.13: A simplified sketch of the set-up and principle for LEEM in diffraction contrast mode. a) the set-up. b) a close-up os the sample surface, c) the diffraction spot chosen for imaging, d) a LEEM image of tin oxide islands on a Pt$_3$Sn(111) surface, from paper v.

LEEM is a microscopy technique that is very surface sensitive thanks to the low energy of the electrons. The set-up has similarities with that used for LEED, and one actually generate LEED patterns also in the LEEM machine. With LEEM, images at a high frame rate (>10fps), and a resolution down to about 2 nm [36] can be recorded while also having information about the structure of the domains imaged, making it a very useful tool for observing surface dynamics. With the related PEEM technique, chemical information can also be obtained about the surface. PEEM uses photo electrons, which carry chemical information. However, the low energy of the electrons makes it necessary to maintain ultra high vacuum (UHV) conditions, and the resolution is not quite atomic-scale. Information on the LEEM instrument and function can be found in Ref. [16], and the textbooks [17, 36].

---

[10] SEM is not surface sensitive, and TEM requires very thin samples.

In order to generate microscopic images of the surface, a number of additional components are needed compared to the LEED set-up. The- LEEM set-up is shown in Figure 4.13 a). An electron beam is generated with an electron gun, just like in the LEED set-up. The electrons are then accelerated by a potential of about -10 to -20 kV. They are sent to a sector field that deflect them toward the sample. Before the beam reaches the sample, it passes through the objective lens (which collimates the beam) and the electrons are decelerated by a strong field while travelling to the sample surface. Aberrations in this field and the objective lens are the main limitations of the resolution [16]. This makes the electron energy low when they reach the surface. At the surface the electrons are backscattered (and diffract) and now contain a real-space image of the surface. As the electrons travel back toward the sector field, the are accelerated to higher energies again, and the sector field deflects the electron beam in a new direction. In the next stage (called the imaging column) the beam is prepared for imaging. Inside of the field lens is the contrast aperture, which allows for blocking out some of the diffraction spots. After a spot is chosen, the filtered beam passes through an electron energy analyser (optional), before reaching the projector system. The projector system magnifies the beam footprint and sends it to a fluorescent screen, where the image is formed. The image is then recorded by a CCD camera.

There are a few different methods to generate the contrast in LEEM images. The most common is amplitude contrast [16], it is this mode that is shown in Figure 4.13. The electron beam undergoes diffraction at the sample surface, meaning that the domains on the surface have scattered the beam at angles depending on the periodicity of their structure. An example is shown in Figure 4.13 b. The substrate with a small unit cell has a diffraction maximum corresponding to a large angle, while the triangular domains with a large unit cell has a diffraction maximum at a smaller angle. These beams correspond to different diffraction spots in the LEED pattern. At the contrast aperture, one of them can be filtered out, meaning that the resulting beam only contains electrons scattered from one of the domains (the triangular domains in Figure 4.13). In the resulting image the triangles will appear bright, while the substrate will appear dark. One can also choose the (0,0) beam, in which case electrons from all domains contribute to the intensity. In this way, height contrast can be obtained, as electrons that scatter from domains of different height will experience a phase shift.

The set-up for LEEM can also be used to generate images using photo electrons coming from the sample. The technique is then called Photo Emission Electron Spectroscopy (PEEM). If x-rays are used the technique is called XPEEM. The photo electrons then follow the same path to the detector as in LEEM. As explained in the XPS section, elements have characteristic photo electron energies, and so elemental contrast can be obtained by using the electron energy analyser. It works in the same way as in XPS. In my work we have used LEEM to follow the growth of tin oxide islands on PtSn surfaces and how they reacted to CO and O_2, among other things.

3.2 Scanning Tunnelling Microscopy (STM) & Atomic Force Microscopy (AFM)

Scanning tunnelling microscopy (STM) and atomic force microscopy (AFM) are both scanning probe microscopy techniques. The "probe" is a tip that is brought into contact (or near contact) with the surface to "feel" its structure, much like a needle reading a vinyl record. They can both reach atomic resolution, but that requires that the tip itself is atomically "sharp" and that its position can be controlled with sub-atomic precision and herein lies the technical challenges with the techniques. The probes are controlled with piezoelectric units, that allow very precise positioning of the tip relative the surface. Piezo-electric materials expand or contract as a response to an applied electrical potential. The expansion is very small, about 1 Å/mV [40], which enables the precision needed. Feedback systems are needed to maintain an appropriate distance between the tip and sample.

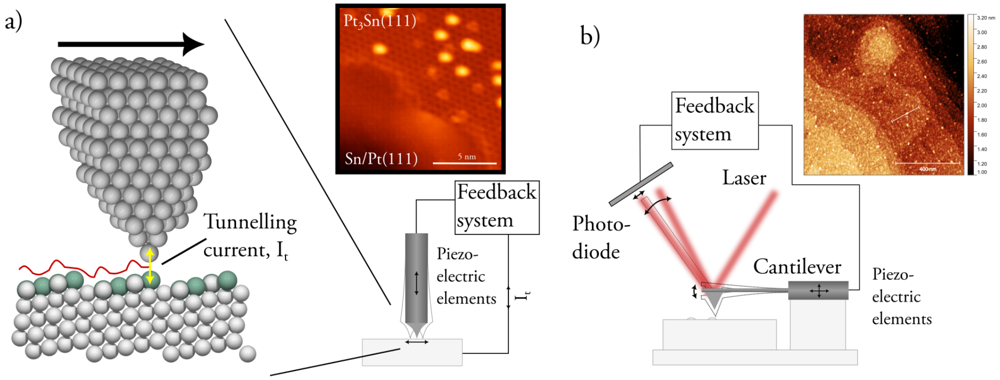

Figure 4.14: Scanning probe techniques. a) The STM set-up. Left shows a model of the tip scanning a surface. The tip is controlled by piezoelectric elements to maintain a constant tunnelling current. Top right shows an STM image of a $Pt_3Sn(111)$ surface. b) The AFM set-up. Top right shows an AFM image of a Sn/Pt(111) surface.

Scanning tunnelling microscopy relies on current flowing between the tip and the sample. As such, it can only be used on samples that conduct electricity. As the name suggests, it relies on the tunnelling effect to pass current. The tunnelling effect is based on that the electron wave functions extend out in space from their atom (or material) and have some, small, probability to be detected some distance away from the atom. If the tip is brought close enough to the surface, the wave functions of some electrons in the sample will extend into the tip and, therefore have a probability of being detected there. There is still an energy barrier to go from the surface to the tip that the electrons cannot overcome, but if they are detected in the tip they don't have to. This is the tunnelling effect: they pass through the barrier like a train though a mountain tunnel [11]. The electron wave functions decay exponentially going away from the atom, which makes the tunnelling probability very sensitive to the tip-surface distance. This provides extraordinary height resolution in

---

[11] It's a little bit like teleportation.

STM. The current that pass also depends on how many electrons are available to tunnel: the density of states of the sample (and the tip). In the Tersoff Hamman theory the tunnelling current is proportional to the energy integrated local density of states, and the bias voltage [111]. This means that what is measured is the density of states of the electrons in the material, not the atomic positions. They often coincide, but not always. An example includes the $Pt_3Sn(111)$ surface, where the platinum atoms have a higher density of states than the tin atoms. Even though the tin atoms protrude slightly from the surface, they appear as hollows when imaged with the STM (see the inset image in Figure 4.14 a for an example). Oxygen atoms in oxides often appear lower is STM images than their physical position would suggest. To generate an image, the tip is swept across the surface by the piezoelectric elements. The feedback system ensures that the current flowing between the tip and the sample is constant (constant current mode) and the tip height adjusts to the topography of the density of states (remember), mapping out an image. As a technique, STM can provide microscopic, atomically resolved images of surfaces that are rivalled by few other techniques, and we have used it extensively to find the structure of the complex tin surface oxides that form on the platinum-tin surface. Typically, it is used in ultra high vacuum conditions, at least when atomic resolution is required. The tip is prone to interference from molecules or other matter binding to it, changing the geometry and reducing the resolution. Acquiring good STM images takes time and patience. The tin oxide island on the front cover of this thesis is a fine example of an STM image.

The other scanning probe technique, atomic force microscopy (AFM), can also provide atomically resolved images. Then it requires special conditions like vacuum, low temperatures etc. It can also be used to get an overview of the surface morphology (so no atomic resolution) without having to bother too much about the conditions: it can be done in air. This is because the AFM tip does not rely on passing any current, making it much less sensitive than the STM. Instead the AFM tip is brought into physical contact (or near contact) with the surface and detecting the repulsion (the ”atomic force”). In this respect it is very much like a needle on the vinyl record. This mode (contact mode) is rough on the surface on an atomic scale, so typically we use other modes. The AFM tip is positioned on a cantilever, and in the non-contact (and tapping) mode the cantilever is oscillated at its resonant frequency above the surface. As the tip is lowered close to the surface, it is repelled by the surface, which affects its oscillation amplitude. This amplitude can be detected and translated to the height of the tip above the surface. This is done by shining a laser on the cantilever and detecting the reflected beam, whose position on the detector will oscillate with the amplitude of the cantilever. Feedback systems ensure that the amplitude is diminished by a set amount, and the tip is scanned across the surface using piezoelectric elements. The result is map of the physical topography of the surface. AFM can be a good complement to STM, as it measures the physical position of the atoms, not the density of states. An example of an AFM image of an Sn/Pt(111) surface in air is shown in Figure 4.14 b. The resolution is far from atomic in that picture, but terraces and clusters can be seen.

4 Computational techniques

4.1 Density Functional Theory (DFT)

Density functional theory (DFT) is a way to calculate the electronic structure of solids, molecules, atoms, and other many-body systems. To calculate the energy exactly, one needs to solve the Schrödinger equation for every particle involved in the material of study. This is not practical, primarily since electron-electron interactions in the material increases the complexity of the calculation enormously. One way around this problem was discovered by Hohenberg and Kohn, who proved that the ground state of a system could be found using a functional of the electron density considered as a whole, rather than considering every electron individually [54]. This made it possible to calculate the ground state energy of materials, but ignored electron-electron interactions. Kohn and Sham developed a method where the electron-electron interactions were treated with additional effective potentials [64]. These two works forms the basis of density functional theory. Finding accurate exchange- and correlation potentials is not easy, however. DFT can be used to calculate whether a proposed structure is energetically favourable, the adsorption energies of molecules on different sites on the surface, reaction barriers for specific steps in a reaction, and much more. The quality DTF calculations have improved with time and provided a trove of useful predictions for materials discovery [82], but a key challenge is still ensuring that the calculations are accurate. DFT calculations are computationally expensive, which especially becomes a problem when dealing with structures with many atoms, and therefore many potential states which have to be considered.

4.2 Machine learning

Machine learning is when a computer is given an ability to learn without being explicitly programmed [44]. It is a useful technique in a number of applications, for example when a data set is too large or complicated for humans to navigate through. This applies to the problem of finding the stable structures of large systems of atoms: the degrees of freedom are many for coming up with new structures to do DFT calculations on, and it is not always clear which new structures are worth trying. One way is to use evolutionary algorithms [81, 114], where new structures are based on random variations of the most stable ones from the previous ”generation”. This calls for a large number of DFT calculations, which is slow. What was done to aid the evolutionary algorithm was to train a model of the energy landscape based on the structures it knew the energy of (through DFT), and extrapolating what the energy would be for the rest of the possible structures [18]. The starting structures were randomly chosen. Of the randomly varied structures generated for the next generation, only those with the lowest energy according to the model were evaluated with DFT, cutting down the number of DFT calculations needed. When the new structures were calculated, they were incorporated into the model, and the model updated with the new information it just obtained. It learned, and with every step the predictive power increased. The model-guided evolutionary algorithm was two orders of magnitude faster than the base evolutionary algorithm in finding the most stable structure. This is how the structure of the (4×4) tin surface oxide was found [75]. The number of atoms that had to be considered and the number of possible configurations was too large for humans or random unguided computer searches to find.

5 Mass spectrometry (MS)

When studying catalysis one of the most important things to know is the gas composition above the sample. Mass spectrometry (MS) is an excellent and relatively simple tool for doing just that. It works by ionising a sample of the gas molecules in the chamber and separate them based on their mass. The mass-charge ratio tells which molecule it is, although there are some molecules that have the same mass. CO and N_2 is one example, as is CH_4 and O. When the molecules are ionised they sometimes split apart into fragments, so for example when O_2 is present one detects mass 32 au. (for ionised O_2) as well as mass 16 au. (atomic oxygen). For CO oxidation the only molecules to consider are CO, O_2 and CO_2, with masses 28 au., 32 au. (and its fragment O at 16 au.), and 44 au. which are all separable. The most common way to separate the ions is to use a quadrupole mass spectrometer (QMS). It works by sending the molecules on a trajectory along four rods with alternating potential [57]. This makes the molecules oscillate along their trajectories giving the oscillation a wavelength based on the charge/mass ratio[12] of the molecule and the frequency of the field oscillation. The formula for the time of flight of the ion is $\tau = \frac{L}{\sqrt{2Z_eU/m}}$ [57] with Z_e the charge, U the field and m the mass. Only molecules at the centre of the trajectory are collected (giving the condition $\tau = n2\pi/\omega$ where n is an integer and ω is the frequency of the field). By choosing the frequency of the field one can choose which mass/charge ratio will be detected. Typically, the machine is set up so that it jumps through some pre-set masses and measures continuously. In my work we have used mass spectrometry to tell when the surface is active, how much CO and O_2 the surfaces are exposed to etc. If one samples all gas in the chamber/reactor, the reactions observed could have occurred at any point in the chamber, not just the sample. One can increase the ratio of gas that has come from the sample surface by sampling the gas just above it with a so-called sniffer. When doing near ambient pressure X-ray Photoelectron Spectroscopy one can conveniently sample the gas coming in through the nozzle of the electron analyser (situated less than a mm above the surface) to get a measurement more likely to be related to the surface processes that are being measured with XPS. This is what we did in paper I and II.

---

[12] usually singly ionised molecules are considered.

Chapter 5

Summary of the research papers

The research papers can be roughly divided into two lines of study. papers I to III are operando spectroscopy studies of PtSn surfaces during CO oxidation, while papers IV to VI focus on ultra high vacuum (UHV) characterisation of the $Pt_3Sn(111)$ surface and the oxide structures that can form on it. Together, they offer an image of the many structures of the PtSn surface, and how it may be related to the catalytic activity.

Paper I: Oxidation of a Platinum–Tin Alloy Surface during Catalytic CO Oxidation

PtSn catalysts has been studied extensively in the past decades, including both surface science and operando studies. The surface science has yielded insights into the structures of PtSn surfaces, and the operando studies have provided evidence for the enhanced activity of PtSn. These operando studies have mostly been done on nanoparticles on porous supports and other complex systems, and a detailed understanding of the PtSn surface in reaction conditions is lacking.

Operando studies on well defined PtSn single crystals are rare but offer a deepened understanding of previous work. We studied a $Pt_3Sn(111)$ single crystal surface in CO oxidation conditions at $\sim$1 mbar pressure while heating step-wise to 300°C, using Near-Ambient Pressure X-ray Photoelectron Spectroscopy (NAP-XPS). The chemical state of the surface and the activity was followed while the CO oxidation was taking place.

We saw that the tin starts oxidising when CO oxidation sets in. The oxide that forms depended on the gas composition, with bulk-like SnO_2 oxide forming in a 1:1 CO:O_2 mixture, and a covering 2D SnO oxide in a 1:10 CO:O_2 mixture. In the 1:10 CO:O_2 mixture self-sustained oscillations were observed, indicating a blocking of active sites by the tin oxide. The results highlighted the dynamical behaviour of the surface structures under reaction conditions, and the need for operando studies.

Paper II: Dynamic Behavior of Tin at Platinum Surfaces during Catalytic CO Oxidation

In Paper I we saw how the formation of tin surface oxide had an effect on the CO oxidation activity of the $Pt_3Sn(111)$ surface. In paper II we wanted to control the amount of oxide that could form, and how large the 2D SnO oxide sheets could grow. This was done by replacing the $Pt_3Sn(111)$ crystal with a Pt(111) and a Pt(223) crystal and depositing a limited amount of tin on them to form surface alloys.

Sn/Pt alloys with 1 and 2 Å tin on them were prepared. The Sn/Pt surface alloys were studied in CO oxidation conditions with NAP-XPS at temperatures up to 400°C and ~1 mbar pressures in 1:1 and 1:10 $CO:O_2$, similar to what was done with the $Pt_3Sn(111)$ in paper I. This time the heating was done continuously and a higher temperature was reached, making it easier to follow the changes on the surface.

On flat Sn/Pt(111) surfaces, covering SnO oxide formed, while a stepped Sn/Pt(223) surface grew bulk-like SnO_2 oxide. The oxides were reduced to metallic or alloyed tin at temperatures close to light-off (~300°C), but only if they expose edge sites to the underlying platinum surface. If the tin coverage was 2 Å, the oxide was covering and did not reduce, while the 1 Å tin surface was not covering and did reduce. Both the flat Sn/Pt(111) surfaces showed higher activity for CO oxidation than the tin-free Pt(111) surface. The activity was attributed to the 2D SnO oxide. The reduction seen for the oxide films was not correlated with any increased activity. The Sn/Pt(223) surface was only more active at low temperature when not much oxide had formed, showing that the SnO_2 did not contribute significantly to the CO oxidation activity.

Paper III: Platinum-Tin surface alloys studied during O_2 exposure, and CO oxidation using grazing-incidence XANES

In paper I and II we saw dynamical and interesting changes on $Pt_3Sn(111)$ and Sn/Pt surfaces during CO oxidation at ~mbar pressures using Near-Ambient Pressure X-ray Photoelectron Spectroscopy (NAP-XPS). Real catalysts are operated at much higher pressures, and we wanted to study the same surfaces as in paper II with a technique that tolerate higher pressures than mbar. We used grazing incidence X-ray Absorption Near Edge Spectroscopy (XANES), which can also provide some structural information.

We prepared the same Sn/Pt surface alloys used in paper II and transported them in vacuum to the x-ray absorption beam line. There, we exposed them to a 1:1 mixture of $CO:O_2$ at ~20 mbar pressure (diluted in He) and temperatures up to 300-350°C, while measuring XNAES. We also exposed the surfaces to pure O_2 and used H_2 to reduce the oxides formed.

Tin on Sn/Pt surfaces oxidises easily to SnO_2 for all surfaces when exposed to O_2. Exposure to CO and O_2 resulted in formation an SnO-like oxide. The spectra of the SnO-like oxide did not match well with bulk SnO, but is similar to simulated spectra of $Sn_{11}O_{12}/Pt_3Sn(111)$ and $Sn_3O_4/Pt_3Sn(111)$ oxides (these oxides are the topic of papers V and VI).

Paper IV: Cleaning and tailoring the $Pt_3Sn(111)$ surface for surface experiments

In order to gain a detailed understanding of the PtSn system, surfaces of high quality need to be prepared. This is not so easy for PtSn, which is difficult to make flat, and suffers from depletion of tin if it is cleaned by argon sputtering.

In paper v the preparation of the $Pt_3Sn(111)$ surface was studied in UHV conditions using Low Energy Electron Diffraction (LEED), Low Energy Electron Microscopy (LEEM) and X-ray Photo Emission Electron Microscopy (XPEEM). The microscopic techniques made it easy to follow and evaluate the effect of the treatments.

A high quality (2 × 2) surface could be obtained by annealing to very high temperatures (above 1340 K), followed by subsequent annealing. The annealing temperature and cooling rate could be used to produce surfaces with varying amounts of surface tin.

Paper V: Oxygen Storage by Tin Oxide Monolayers on $Pt_3Sn(111)$

The SnO-like surface oxides that form on PtSn have attracted some interest in the past because of their proposed role in the CO oxidation reaction. Two of them, a surface oxide with (4 × 4) periodicity and a related $(2m \times 2n)$ oxide were the focus of paper v. The structure of the (4 × 4) oxide was solved previously, but the $(2m \times 2n)$ oxide is more complicated and motivated a more detailed investigation.

The (4 × 4) and $(2m \times 2n)$ oxides were formed on the $Pt_3Sn(111)$ surface and studied with scanning tunnelling microscopy (STM), Low Energy Electron Diffraction and Microscopy LEED/LEEM. It is possible to transition between these two phases using CO and O_2 at low pressures. Density Functional Theory (DFT) was used to support the experimental findings.

The transition from the (4 × 4) $Sn_{11}O_{12}/Pt_3Sn(111)$ oxide to the $(2m \times 2n)$ oxide proceeded through exposure to oxygen at sufficient temperatures, although the oxidation was slow. The $(2m \times 2n)$ oxide was found to be more oxygen rich than the (4 × 4) oxide. The $(2m \times 2n)$ oxide incorporates oxygen at the interface and the substrate to form $Sn_3O_4/Pt_3Sn(111)$, an ability attributed to the asymmetrical coordination state of Sn^{2+}. The $(2m \times 2n)$ was very easily reduced to the (4 × 4) by exposing the surface to CO at 5×10^{-5} mbar. This oxygen storage mechanism was proposed to be potentially important for the CO oxidation ability of Pt_3Sn.

Paper vi: Growth, structure, and morphology of ultra-thin tin oxide phases forming on $Pt_3Sn(111)$ upon exposure to oxygen

With the background of paper v, it is of interest to map out how the $Pt_3Sn(111)$ surface responds to oxygen in different conditions. This is what was done in paper vi, and the formation and characteristics of the $(2m \times 2n)$ surface oxide was further investigated.

The $Pt_3Sn(111)$ surface was exposed to oxygen at different temperatures and studied with LEED, LEEM, SXRD, XPS and STM. We could see how the oxide developed under different conditions with LEEM/LEED, while STM provided detailed microscopic images. The XPS spectra provided the chemical composition of the (4×4) and $(2m \times 2n)$ surface oxides.

The $(2m \times 2n)$ was found to consist of several domains of a complex structure. The periodicity across the stripes in the oxide varies, creating a non-homogeneous surface. The (4×4) and $(2m \times 2n)$ oxides are closely related. The XPS seems to suggest that the extra oxygen in the $(2m \times 2n)$ oxide is at the interface between the (4×4) oxide (or a similar oxide) and the $Pt_3Sn(111)$ substrate. This was hypothesised in paper v, but calculations would be needed to be certain.

Chapter 6

Outlook

This thesis work can be divided roughly in two lines of work: we have studied platinum tin surfaces in ultra high vacuum conditions where we seen the ordered tin surface oxides and how they interact with gases, and we have done operando studies of platinum-tin surfaces during CO oxidation in millibar pressures. There are several things that would be interesting to do that relates directly to our previous work.

The (4×4) $Sn_{11}O_{12}/Pt_3Sn(111)$ surface oxide is characterised, but the structure of the related $(2m \times 2n)$ surface oxide is not solved yet. The unit cell of the $(2m \times 2n)$ oxide is larger than for the (4×4) oxide, and also contains a mixture of domains. This made it difficult to find the right structure with theory. Characterising the $(2m \times 2n)$ oxide with surface x-ray diffraction with rod scans would aid in finding the right structure. If x-ray absorption fine structure spectra of good quality that could be proven to be from (only) the (4×4) and $(2m \times 2n)$ oxides, they could also provide information about their structure and be useful for higher pressure studies.

We have expanded our knowledge of these surface oxides in vacuum conditions, but platinum-tin catalysts are used in real conditions of one or several bars. If the (4×4) and $(2m \times 2n)$ surface oxides could be detected at higher pressures, it could mean that they play a role for the real catalyst. The diffraction patterns of the two surface oxides are known, so one could try to do a high energy surface x-ray diffraction experiment at pressures going from millibar up to 1 bar, for example, and see if the oxides can be detected. The next step could be to study them in reaction conditions. x-ray absorption could also be used for this purpose as it is a technique that can be used at higher pressure. For that to work, a high quality characterisation of the EXAFS would be necessary, as suggested in the previous paragraph. Studies such as these could help link the UHV studies to real conditions and help bridge the pressure gap.

Looking further ahead, there are many paths to go down. There are more tin surface oxides on platinum than the (4×4) and $(2m\times2n)$, for example the nano islands and the related incommensurate oxide studied by Batzill [11] that formed at more oxidising conditions. They are possible candidates for oxygen storage and release that may be relevant at more realistic conditions. Ultra high vacuum characterisation (with for example XPS, XAS, XRD) of these phases coupled with theory would be a good start, followed by operando studies later. There are also other reactions than CO oxidation that platinum-tin is used for. Electro-oxidation of alcohols is one, where CO can be expected to show up as an intermediate species. Studying how the tin surface oxides (if they form) behave in an electro-chemical environment could be very interesting. It will require techniques that can be used in such an environment. XPS is one, as is XRD and XAS.

Another path to head down is to study tin oxides on other materials. Tin alloys in a similar way to nickel as it does to platinum, and the formation of tin oxides have been shown to play a similar role as in platinum-tin [84, 80, 95], such as protecting the nickel catalyst from carbon poisoning, lowering the binding energy of CO etc. One of the issues with platinum-tin is the high price of platinum, and so the properties of Ni_3Sn could be looked into with the background knowledge acquired about platinum-tin. Tin surface oxides have also been studied on Au(111) surfaces for CO_2 activation [62]. The goal is hydrogenation of CO_2 to form fuels and other valuable chemicals, and the tin was found to re-oxidise during reaction. Also here the knowledge of tin oxides gained from platinum-tin surfaces could guide experiments and the results be compared to the results from platinum-tin.

Chapter 7

References

[1] J. Als-Nielsen and D. McMorrow. *Elements of Modern X-ray Physics*. Wiley, 2011.

[2] J. Araña, P. Ramirez de la Piscina, J. Llorca, J. Sales, N. Homs, and J. L. G. Fierro. Bimetallic Silica-Supported Catalysts Based on Ni–Sn, Pd–Sn, and Pt–Sn as Materials in the CO Oxidation Reaction. *Chemistry of Materials*, 10(5):1333–1342, 1998.

[3] M. Arenz, V. Stamenkovic, B.B. Blizanac, K.J. Mayrhofer, N.M. Markovic, and P.N. Ross. Carbon-supported Pt–Sn electrocatalysts for the anodic oxidation of H_2, CO, and H_2/CO mixtures.: Part II: The structure–activity relationship. *Journal of Catalysis*, 232(2):402–410, 2005.

[4] A. Atrei, U. Bardi, G. Rovida, M. Torrini, M. Hoheisel, and S. Speller. Test of structural models for the (4×4) phase formed by oxygen adsorption on the Pt_3Sn(111) surface. *Surface Science*, 526(1):193–200, 2003.

[5] A. Atrei, U. Bardi, G. Rovida, M. Torrini, E. Zanazzi, and P. N. Ross. Structure of the (001)- and (111)-oriented surfaces of the ordered fcc Pt_3Sn alloy by low-energy-electron-diffraction intensity analysis. *Phys. Rev. B*, 46:1649–1654, Jul 1992.

[6] A Atrei, U Bardi, M Torrini, E Zanazzi, G Rovida, H Kasamura, and M Kudo. Structure of a non-bulk termination of the clean Pt_3Sn(111) surface: a study by low-energy electron diffraction and X-ray photoelectron diffraction. *Journal of Physics: Condensed Matter*, 5(14):L207, apr 1993.

[7] A. Atrei, U. Bardi, J.X. Wu, E. Zanazzi, and G. Rovida. LEED crystallographic investigation of ultrathin films formed by deposition of Sn on the Pt(111) surface. *Surface Science*, 290(3):286–294, 1993.

[8] Stephanus Axnanda, Wei-Ping Zhou, and Michael G. White. CO oxidation on nanostructured SnO_x/Pt(111) surfaces: unique properties of reduced SnO_x. *Phys. Chem. Chem. Phys.*, 14:10207–10214, 2012.

[9] Stephanus Axnanda, Zhongwei Zhu, Weiping Zhou, Baohua Mao, Rui Chang, Sana Rani, Ethan Crumlin, Gabor Somorjai, and Zhi Liu. In Situ Characterizations of Nanostructured SnO_x/Pt(111) Surfaces Using Ambient-Pressure XPS (APXPS) and High-Pressure Scanning Tunneling Microscopy (HPSTM). *The Journal of Physical Chemistry C*, 118(4):1935–1943, 2014.

[10] U Bardi. The atomic structure of alloy surfaces and surface alloys. *Reports on Progress in Physics*, 57(10):939, oct 1994.

[11] Matthias Batzill, David E. Beck, Dmitri Jerdev, and Bruce E. Koel. Tin-oxide overlayer formation by oxidation of Pt–Sn(111) surface alloys. *Journal of Vacuum Science & Technology A*, 19(4):1953–1958, 2001.

[12] Matthias Batzill, David E. Beck, and Bruce E. Koel. Self-organized molecular-sized, hexagonally ordered SnO_x nanodot superlattices on Pt(111). *Applied Physics Letters*, 78(18):2766–2768, 04 2001.

[13] Matthias Batzill, David E. Beck, and Bruce E. Koel. Structure of monolayer tin oxide films on Pt(111) formed using NO_2 as an efficient oxidant. *Phys. Rev. B*, 64:245402, Nov 2001.

[14] Matthias Batzill and Ulrike Diebold. The surface and materials science of tin oxide. *Progress in Surface Science*, 79(2):47 – 154, 2005.

[15] Matthias Batzill, Jooho Kim, David E. Beck, and Bruce E. Koel. Epitaxial growth of tin oxide on Pt(111): Structure and properties of wetting layers and SnO_2 crystallites. *Phys. Rev. B*, 69:165403, Apr 2004.

[16] Ernst Bauer. Low energy electron microscopy. *Reports on Progress in Physics*, 57(9):895, sep 1994.

[17] Ernst Bauer. *Surface Microscopy with Low Energy Electrons*. Springer New York, NY, 2014.

[18] Malthe K. Bisbo and Bjørk Hammer. Efficient Global Structure Optimization with a Machine-Learned Surrogate Model. *Phys. Rev. Lett.*, 124:086102, Feb 2020.

[19] R. Burch. Platinum-tin reforming catalysts: I. The oxidation state of tin and the interaction between platinum and tin. *Journal of Catalysis*, 71(2):348–359, 1981.

[20] S. Calvin. *XAFS for Everyone*. Taylor & Francis, 2013.

[21] W.C.A.N. Ceelen, A.W. Denier van der Gon, M.A. Reijme, H.H. Brongersma, I. Spolveri, A. Atrei, and U. Bardi. Domain structure, segregation and morphology of the $Pt_3Sn(111)$ surface. *Surface Science*, 406(1):264 – 278, 1998.

[22] D. Chandler. *Introduction to Modern Statistical Mechanics*. Oxford University Press, 1987.

[23] I. Chorkendorff and J.W. Niemantsverdriet. *Concepts of Modern Catalysis and Kinetics*. Wiley, 2017.

[24] Kajsa Sigfridsson Clauss, Konstantin Klementiev, Justus Just, Susan Nehzati, Mahesh Ramakrishnan, Dörthe Haase, Stefan Carlson, and Stuart Ansell. Balder Beamline - MAX IV beamline review report. Technical report, MAX IV, 2023.

[25] Randy D Cortright, Josephine M Hill, and James A Dumesic. Selective dehydrogenation of isobutane over supported Pt/Sn catalysts. *Catalysis Today*, 55(3):213–223, 2000.

[26] C Creemers and S Helfensteyn. MAM modelling of the segregation and ordering at the $Pt_3Sn(111)$ surface. *Applied Surface Science*, 167(3):216–229, 2000.

[27] C. Davisson and L. H. Germer. Diffraction of Electrons by a Crystal of Nickel. *Phys. Rev.*, 30:705–740, Dec 1927.

[28] Louis de Broglie. XXXV. A tentative theory of light quanta . *The London, Edinburgh, and Dublin Philosophical Magazine and Journal of Science*, 47(278):446–458, 1924.

[29] David Degerman, Peter Amann, Christopher M. Goodwin, Patrick Lömker, Hsin-Yi Wang, Markus Soldemo, Mikhail Shipilin, Christoph Schlueter, and Anders Nilsson. Operando X-ray Photoelectron Spectroscopy for High-Pressure Catalysis Research Using the POLARIS Endstation. *Synchrotron Radiation News*, 35(3):11–18, 2022.

[30] Wenxin Du, Guangxing Yang, Emily Wong, N. Aaron Deskins, Anatoly I. Frenkel, Dong Su, and Xiaowei Teng. Platinum-Tin Oxide Core–Shell Catalysts for Efficient Electro-Oxidation of Ethanol. *Journal of the American Chemical Society*, 136(31):10862–10865, Aug 2014.

[31] Céline Dupont, Yvette Jugnet, Françoise Delbecq, and David Loffreda. Restructuring of the $Pt_3Sn(111)$ surfaces induced by atomic and molecular oxygen from first principles. *The Journal of Chemical Physics*, 130(12):124716, 2009.

[32] Céline Dupont, Yvette Jugnet, Françoise Delbecq, and David Loffreda. Mediatory role of tin in the catalytic performance of tailored platinum–tin alloy surfaces for carbon monoxide oxidation. *Journal of Catalysis*, 273(2):211–220, 2010.

[33] Céline Dupont, David Loffreda, Françoise Delbecq, and Yvette Jugnet. Vibrational Study of CO Chemisorption on the $Pt_3Sn(111)$-(2 × 2) Surface. *The Journal of Physical Chemistry C*, 111(24):8524–8531, 2007.

[34] Ph. Durussel, R. Massara, and P. Feschotte. Le système binaire Pt-Sn. *Journal of Alloys and Compounds*, 215(1):175–179, 1994.

[35] A. Eichler and J. Hafner. Reaction channels for the catalytic oxidation of CO on Pt(111). *Phys. Rev. B*, 59:5960–5967, Feb 1999.

[36] J. I. Flege, W. X. Tang, and M. S. Altman. *Low-Energy Electron Microscopy*, pages 1–22. John Wiley & Sons, Ltd, 2012.

[37] Monica Galeotti, Andrea Atrei, Ugo Bardi, Gianfranco Rovida, and Marco Torrini. Surface alloying at the $Sn_3Pt(111)$ interface: a study by x-ray photoelectron diffraction. *Surface Science*, 313(3):349 – 354, 1994.

[38] C. Gallis, B. Legrand, and G. Tréglia. On the "exotic" behaviour of the Pt-Sn system. *Surface Science*, 377-379:1033–1037, 1997. European Conference on Surface Science.

[39] N.D. Gangal, N.M. Gupta, and R.M. Iyer. Microcalorimetric study of the interaction of CO, O2, and CO + O_2 with Pt/SnO_2 and SO_2 catalysts. *Journal of Catalysis*, 126(1):13–25, 1990.

[40] Attard Gary and Barnes Colin. *Surfaces*. Oxford University Press, 06 1998.

[41] Hubert A. Gasteiger. On the Differences in the Reaction Mechanism for CO and CO/H_2 Electrooxidation on PtRu and PtSn Alloy Electrodes. LBNL Report LBNL-40196, Lawrence Berkeley National Laboratory, 1997. https://escholarship.org/uc/item/4r96g572.

[42] Hubert A. Gasteiger, Nenad M. Markovic, and Philip N. Ross. Electrooxidation of CO and H_2/CO Mixtures on a Well-Characterized Pt_3Sn Electrode Surface. *The Journal of Physical Chemistry*, 99(22):8945–8949, Jun 1995.

[43] Hubert A. Gasteiger, Nenad M. Marković, and Philip N. Ross. Structural effects in electrocatalysis: electrooxidation of carbon monoxide on Pt_3Sn single-crystal alloy surfaces. *Catalysis Letters*, 36(1):1–8, Mar 1996.

[44] A. Géron. *Hands-on Machine Learning with Scikit-Learn, Keras, and TensorFlow: Concepts, Tools, and Techniques to Build Intelligent Systems*. O'Reilly Media, Incorporated, 2019.

[45] A. H. Haner, P. N. Ross, U. Bardi, and A. Atrei. Surface composition determination of Pt–Sn alloys by chemical titration with carbon monoxide. *Journal of Vacuum Science & Technology A*, 10(4):2718–2722, 07 1992.

[46] Alexandra N. Haner, Philip N. Ross, and Ugo Bardi. The surface structure and composition of <111> and <100> oriented single crystals of the ordered alloy Pt$_3$Sn. *Surface Science*, 249(1):15–20, 1991.

[47] Alexandra N. Haner, Philip N. Ross, and Ugo Bardi. The surface structure and composition of the low index single crystal faces of the ordered alloy Pt$_3$Sn. *Catalysis Letters*, 8(1):1–7, Jan 1991.

[48] Brian E. Hayden, Michael E. Rendall, and Oliver South. Electro-oxidation of Carbon Monoxide on Well-Ordered Pt(111)/Sn Surface Alloys. *Journal of the American Chemical Society*, 125(25):7738–7742, 2003. PMID: 12812515.

[49] Brian E. Hayden, Michael E. Rendall, and Oliver South. The stability and electro-oxidation of carbon monoxide on model electrocatalysts: Pt(111)–Sn(2×2) and Pt(111)–Sn($\sqrt{3}\times\sqrt{3}$)R30°. *Journal of Molecular Catalysis A: Chemical*, 228(1):55–65, 2005. Proceedings of the Third San Luis Symposium on Surfaces, Interfaces and Catalysis.

[50] Josephine M Hill, R.D Cortright, and J.A Dumesic. Silica- and L-zeolite-supported Pt, Pt/Sn and Pt/Sn/K catalysts for isobutane dehydrogenation. *Applied Catalysis A: General*, 168(1):9–21, 1998.

[51] Gar B Hoflund and Douglas A Asbury. ESCA study of the oxidation of platinum-tin (Pt$_3$Sn). 2. Exposure to air. *Langmuir*, 2(6):695–697, 1986.

[52] Gar B. Hoflund, Douglas A. Asbury, Piotr Kirszensztejn, and Herbert A. Laitinen. An ISS and AES examination of the interaction of oxygen with platinum-tin alloy. *Surface Science*, 161(2):L583–L590, 1985.

[53] M. Hoheisel, S. Speller, W. Heiland, A. Atrei, U. Bardi, and G. Rovida. Adsorption of oxygen on Pt$_3$Sn(111) studied by scanning tunneling microscopy and x-ray photoelectron diffraction. *Phys. Rev. B*, 66:165416, Oct 2002.

[54] P. Hohenberg and W. Kohn. Inhomogeneous Electron Gas. *Phys. Rev.*, 136:B864–B871, Nov 1964.

[55] H. Hopster and H. Ibach. Adsorption of CO on Pt(111) and Pt 6(111) × (111) studied by high resolution electron energy loss spectroscopy and thermal desorption spectroscopy. *Surface Science*, 77(1):109–117, 1978.

[56] Stefan Hüfner. *Photoelectron Spectroscopy.* Springer Berlin, Heidelberg, 1988. `https://link.springer.com/book/10.1007/978-3-662-03150-6`(visited 2024-04-15).

[57] Harald Ibach. *Physics of Surfaces and Interfaces.* Springer Berlin, Heidelberg, 2006.

[58] Dmitri I. Jerdev and Bruce E. Koel. Oxidation of ordered Pt–Sn surface alloys by O_2. *Surface Science*, 492(1):106 – 114, 2001.

[59] Luhua Jiang, Gongquan Sun, Shiguo Sun, Jianguo Liu, Shuihua Tang, Huanqiao Li, Bing Zhou, and Qin Xin. Structure and chemical composition of supported Pt–Sn electrocatalysts for ethanol oxidation. *Electrochimica Acta*, 50(27):5384–5389, 2005.

[60] Yvette Jugnet, David Loffreda, Céline Dupont, Françoise Delbecq, Eric Ehret, Francisco J. Cadete Santos Aires, Bongjin S. Mun, Funda Aksoy Akgul, and Zhi Liu. Promoter Effect of Early Stage Grown Surface Oxides: A Near-Ambient-Pressure XPS Study of CO Oxidation on PtSn Bimetallics. *The Journal of Physical Chemistry Letters*, 3(24):3707–3714, 2012. PMID: 26291100.

[61] Jongkeun Jung, Sungwoo Kang, Laurent Nicolaï, Jisook Hong, Ján Minár, Inkyung Song, Wonshik Kyung, Soohyun Cho, Beomseo Kim, Jonathan D. Denlinger, Francisco José Cadete Santos Aires, Eric Ehret, Philip Ross, Jihoon Shim, Slavomir Nemšák, Doyoung Noh, Seungwu Han, Changyoung Kim, and Bongjin Simon Mun. Understanding the Role of Electronic Effects in CO on the Pt–Sn Alloy Surface via Band Structure Measurements. *ACS Catalysis*, 12(1):219–225, 2022.

[62] Jindong Kang, Ning Rui, Rina Rosales, Yi Tian, Sanjaya D. Senanayake, and José A. Rodriguez. Understanding the Surface Structure and Catalytic Activity of SnO_x/Au(111) Inverse Catalysts for CO_2 and H_2 Activation. *The Journal of Physical Chemistry C*, 126(10):4862–4870, 2022.

[63] C. Kittel, P. McEuen, and John Wiley & Sons. *Introduction to Solid State Physics*. John Wiley & Sons, 2015.

[64] W. Kohn and L. J. Sham. Self-Consistent Equations Including Exchange and Correlation Effects. *Phys. Rev.*, 140:A1133–A1138, Nov 1965.

[65] Laura Y Kraya, Guangzhi F Liu, Xiaobo He, and Bruce E Koel. Structures and Reactivities of Tin Oxide on Pt (111) Studied by Ambient Pressure X-ray Photoelectron Spectroscopy (APXPS). *Topics in Catalysis*, 59(5):497–505, 2016.

[66] J. Kuntze, S. Speller, W. Heiland, A. Atrei, I. Spolveri, and U. Bardi. Reconstruction and dislocation network formation of the (111) surface of the ordered alloy Pt_3Sn. *Phys. Rev. B*, 58:R16005–R16008, Dec 1998.

[67] C Lamy, S Rousseau, E.M Belgsir, C Coutanceau, and J.-M Léger. Recent progress in the direct ethanol fuel cell: development of new platinum–tin electrocatalysts. *Electrochimica Acta*, 49(22):3901–3908, 2004. The role of electrochemistry in the sustained development of modern societies.

[68] Irving Langmuir. THE ADSORPTION OF GASES ON PLANE SURFACES OF GLASS, MICA AND PLATINUM. *Journal of the American Chemical Society*, 40(9):1361–1403, 1918.

[69] Irving Langmuir. The mechanism of the catalytic action of platinum in the reactions 2CO + O_2= $2CO_2$ and $2H_2$+ O_2= $2H_2O$. *Trans. Faraday Soc.*, 17:621–654, 1922.

[70] Meng-Sheng Liao, Carlos R. Cabrera, and Yasuyuki Ishikawa. A theoretical study of CO adsorption on Pt, Ru and Pt–M (M=Ru, Sn, Ge) clusters. *Surface Science*, 445(2):267–282, 2000.

[71] Yougui Liao. Practical electron microscopy and database. *An Online Book*, 2006.

[72] P. Liu, A. Logadottir, and J.K. Nørskov. Modeling the electro-oxidation of CO and H_2/CO on Pt, Ru, PtRu and Pt_3Sn. *Electrochimica Acta*, 48(25):3731–3742, 2003. Electrocatalysis:From Theory to Industrial Applications.

[73] Yi Liu, Dongguo Li, Vojislav R. Stamenkovic, Stuart Soled, Juan D. Henao, and Shouheng Sun. Synthesis of Pt_3Sn Alloy Nanoparticles and Their Catalysis for Electro-Oxidation of CO and Methanol. *ACS Catalysis*, 1(12):1719–1723, Dec 2011.

[74] S.M. McMurry. *Quantum Mechanics*. Pearson Education. Addison-Wesley, 1994.

[75] Lindsay R. Merte, Malthe Kjær Bisbo, Igor Sokolović, Martin Setvín, Benjamin Hagman, Mikhail Shipilin, Michael Schmid, Ulrike Diebold, Edvin Lundgren, and Bjørk Hammer. Structure of an Ultrathin Oxide on Pt_3Sn(111) Solved by Machine Learning Enhanced Global Optimization**. *Angewandte Chemie International Edition*, 61(25):e202204244, 2022.

[76] William D. Michalak, James M. Krier, Selim Alayoglu, Jae-Yoon Shin, Kwangjin An, Kyriakos Komvopoulos, Zhi Liu, and Gabor A. Somorjai. CO oxidation on PtSn nanoparticle catalysts occurs at the interface of Pt and Sn oxide domains formed under reaction conditions. *Journal of Catalysis*, 312:17–25, 2014.

[77] Alina Moscu, Laurent Veyre, Chloé Thieuleux, Frederic Meunier, and Yves Schuurman. CO PROX over Pt–Sn/Al_2O_3: A combined kinetic and in situ DRIFTS study. *Catalysis Today*, 258:241–246, 2015. Selected contributions in the field of heterogeneous catalysis and photocatalysis that were presented at the 8th International Conference on Environmental Catalysis (ICEC 2014).

[78] Falko P. Netzer, Francesco Allegretti, and Svetlozar Surnev. Low-dimensional oxide nanostructures on metals: Hybrid systems with novel properties. *Journal of Vacuum Science & Technology B*, 28(1):1–16, 2010.

[79] Matthew Newville. *Fundamentals of XAFS*. University of Chicago, Chicago, IL, July 2004.

[80] Eranda Nikolla, Johannes Schwank, and Suljo Linic. Comparative study of the kinetics of methane steam reforming on supported Ni and Sn/Ni alloy catalysts: The impact of the formation of Ni alloy on chemistry. *Journal of Catalysis*, 263(2):220–227, 2009.

[81] Artem R. Oganov and Colin W. Glass. Crystal structure prediction using ab initio evolutionary techniques: Principles and applications. *The Journal of Chemical Physics*, 124(24):244704, 06 2006.

[82] Artem R. Oganov, Chris J. Pickard, Qiang Zhu, and Richard J. Needs. Structure prediction drives materials discovery. *Nature Reviews Materials*, 4(5):331–348, May 2019.

[83] S.H. Overbury, D.R. Mullins, M.T. Paffett, and B.E. Koel. Surface structure determination of Sn deposited on Pt(111) by low energy alkali ion scattering. *Surface Science*, 254(1):45–57, 1991.

[84] Celestino Padeste, David L. Trimm, and Robert N. Lamb. Characterization of Sn doped Ni/Al_2O_3 steam reforming catalysts by XPS. *Catalysis Letters*, 17(3):333–339, Sep 1993.

[85] M T Paffett, S C Gebhard, R G Windham, and B E Koel. Chemisorption of CO, H_2 , and O_2 on ordered Sn/Pt(111) surface alloys. *Journal of Physical Chemistry; (USA)*, 94(17), 8 1990.

[86] M.T. Paffett and R.G. Windham. Surface modification of Pt(111) by Sn adatoms: Evidence for the formation of ordered overlayers and surface alloys. *Surface Science*, 208(1):34 – 54, 1989.

[87] Bullion vault. `https://www.bullionvault.com/platinum-price-chart.do`. Accessed: 2024-05-22.

[88] V. Radmilovic, T.J. Richardson, S.J. Chen, and P.N. Ross. Carbon-supported Pt–Sn electrocatalysts for the anodic oxidation of H_2, CO, and H_2/CO mixtures. Part I. Microstructural characterization. *Journal of Catalysis*, 232(1):199–209, 2005.

[89] John J Rehr, Joshua J Kas, Micah P Prange, Adam P Sorini, Yoshinari Takimoto, and Fernando Vila. Ab initio theory and calculations of X-ray spectra. *Comptes Rendus Physique*, 10(6):548–559, 2009.

[90] John J Rehr, Joshua J Kas, Fernando D Vila, Micah P Prange, and Kevin Jorissen. Parameter-free calculations of X-ray spectra with FEFF9. *Physical Chemistry Chemical Physics*, 12(21):5503–5513, 2010.

[91] Ruben Rizo, Elena Pastor, and Marc T.M. Koper. CO electrooxidation on Sn-modified Pt single crystals in acid media. *Journal of Electroanalytical Chemistry*, 800:32–38, 2017. Special Issue in honor of Masatoshi Osawa.

[92] J. A. Rodriguez, S. Ma, P. Liu, J. Hrbek, J. Evans, and M. Pérez. Activity of CeO_x and TiO_x Nanoparticles Grown on Au(111) in the Water-Gas Shift Reaction. *Science*, 318(5857):1757–1760, 2007.

[93] Philip N. Ross. Trends in the bonding of CO to the surfaces of Pt_3M alloys (M=Ti, Co, and Sn). *Journal of Vacuum Science & Technology A*, 10(4):2546–2550, 07 1992.

[94] H. H. Rotermund, V. Penka, L. A. De Louise, and C. R. Brundle. Oxygen interaction with Pd_3Sn: X-ray photoelectron spectroscopy and secondary ion mass spectrometry. *Journal of Vacuum Science & Technology A*, 5(4):1198–1202, 1987.

[95] Souheil Saadi, Berit Hinnemann, Stig Helveg, Charlotte C. Appel, Frank Abild-Pedersen, and Jens K. Nørskov. First-principles investigations of the Ni_3Sn alloy at steam reforming conditions. *Surface Science*, 603(5):762–770, 2009.

[96] Najat A. Saliba, Yi-Li Tsai, and Bruce E. Koel. Oxidation of Ordered Sn/Pt(111) Surface Alloys and Thermal Stability of the Oxides Formed. *The Journal of Physical Chemistry B*, 103(9):1532–1541, 1999.

[97] Martin Schmid, Hans-Peter Steinrück, and J. Michael Gottfried. A new asymmetric Pseudo-Voigt function for more efficient fitting of XPS lines. *Surface and Interface Analysis*, 46(8):505–511, 2014.

[98] M. M. Schubert, M. J. Kahlich, G. Feldmeyer, M. Hüttner, S. Hackenberg, H. A. Gasteiger, and R. J. Behm. Bimetallic PtSn catalyst for selective CO oxidation in H_2-rich gases at low temperatures. *Physical Chemistry Chemical Physics*, 3(6):1123–1131, 2001.

[99] Masami Shibata and Nagakazu Furuya. Catalysis by ad-atoms: Part II. Enhancement of CO oxidation on Pt catalysts modified by Sn ad-atoms in the gaseous phase. *Journal of Electroanalytical Chemistry and Interfacial Electrochemistry*, 269(1):217–221, 1989.

[100] T.E Shubina and M.T.M Koper. Quantum-chemical calculations of CO and OH interacting with bimetallic surfaces. *Electrochimica Acta*, 47(22):3621–3628, 2002.

[101] Kai Siegbahn. Electron spectroscopy for atoms, molecules, and condensed matter. *Rev. Mod. Phys.*, 54:709–728, Jul 1982.

[102] Jagdeep Singh, Ryan C. Nelson, Brian C. Vicente, Susannah L. Scott, and Jeroen A. van Bokhoven. Electronic structure of alumina-supported monometallic Pt and

bimetallic PtSn catalysts under hydrogen and carbon monoxide environment. *Phys. Chem. Chem. Phys.*, 12:5668–5677, 2010.

[103] H. L. Skriver. Electronic structure of the intermetallic compound Pt_3Sn. *Phys. Rev. B*, 14:5187–5197, Dec 1976.

[104] Vaclav Smil. Detonator of the population explosion. *Nature*, 400(6743):415–415, Jul 1999.

[105] V. Stamenković, M. Arenz, B.B. Blizanac, K.J.J. Mayrhofer, P.N. Ross, and N.M. Marković. In situ CO oxidation on well characterized Pt_3Sn(hkl) surfaces: A selective review. *Surface Science*, 576(1):145–157, 2005.

[106] Vojislav R. Stamenković, Matthias Arenz, Christopher A. Lucas, Mark E. Gallagher, Philip N. Ross, and Nenad M. Marković. Surface Chemistry on Bimetallic Alloy Surfaces: Adsorption of Anions and Oxidation of CO on Pt_3Sn(111). *Journal of the American Chemical Society*, 125(9):2736–2745, 2003. PMID: 12603163.

[107] Y.-N. Sun, Z.-H. Qin, M. Lewandowski, E. Carrasco, M. Sterrer, S. Shaikhutdinov, and H.-J. Freund. Monolayer iron oxide film on platinum promotes low temperature CO oxidation. *Journal of Catalysis*, 266(2):359–368, 2009.

[108] Ying-Na Sun, Zhi-Hui Qin, Mikolaj Lewandowski, Sarp Kaya, Shamil Shaikhutdinov, and Hans-Joachim Freund. When an Encapsulating Oxide Layer Promotes Reaction on Noble Metals: Dewetting and In situ Formation of an “Inverted” FeO_x/Pt Catalyst. *Catalysis Letters*, 126(1):31–35, Nov 2008.

[109] SJ Tauster. Strong metal-support interactions. *Accounts of Chemical Research*, 20(11):389–394, 1987.

[110] SJ Tauster, SC Fung, and Rl L Garten. Strong metal-support interactions. Group 8 noble metals supported on titanium dioxide. *Journal of the American Chemical Society*, 100(1):170–175, 1978.

[111] J. Tersoff and D. R. Hamann. Theory of the scanning tunneling microscope. *Phys. Rev. B*, 31:805–813, Jan 1985.

[112] Wolfgang Unger and Dénes Marton. A SIMS and XPS examination of low-pressure oxygen adsorption on Pt_3Sn: Oxygen uptake and surface characteristics. *Surface Science*, 218(2):L467–L475, 1989.

[113] R.A. Van Santen and W.M.H. Sachtler. A theory of surface enrichment in ordered alloys. *Journal of Catalysis*, 33(2):202–209, 1974.

[114] Lasse B. Vilhelmsen and Bjørk Hammer. A genetic algorithm for first principles global structure optimization of supported nano structures. *The Journal of Chemical Physics*, 141(4):044711, 07 2014.

[115] Qing Wang, Didier Tichit, Frederic Meunier, and Hazar Guesmi. Combined DRIFTS and DFT Study of CO Adsorption and Segregation Modes in Pt–Sn Nanoalloys. *The Journal of Physical Chemistry C*, 124(18):9979–9989, 2020.

[116] Ramchandra M Watwe, Randy D Cortright, Manos Mavrikakis, Jens K Nørskov, and James A Dumesic. Density functional theory studies of the adsorption of ethylene and oxygen on Pt (111) and Pt3Sn (111). *The Journal of Chemical Physics*, 114(10):4663–4668, 2001.

[117] Wei-Ping Zhou, Wei An, Dong Su, Robert Palomino, Ping Liu, Michael G. White, and Radoslav R. Adzic. Electrooxidation of Methanol at SnO_x–Pt Interface: A Tunable Activity of Tin Oxide Nanoparticles. *The Journal of Physical Chemistry Letters*, 3(22):3286–3290, 2012.

[118] Wei-Ping Zhou, Stephanus Axnanda, Michael G. White, Radoslav R. Adzic, and Jan Hrbek. Enhancement in Ethanol Electrooxidation by SnO_x Nanoislands Grown on Pt(111): Effect of Metal Oxide–Metal Interface Sites. *The Journal of Physical Chemistry C*, 115(33):16467–16473, 2011.

[119] Suyun Zhu, Mattia Scardamaglia, Jan Kundsen, Rami Sankari, Hamed Tarawneh, Robert Temperton, Louisa Pickworth, Filippo Cavalca, Chunlei Wang, Héloïse Tissot, Jonas Weissenrieder, Benjamin Hagman, Johan Gustafson, Sarp Kaya, Fredrik Lindgren, Ida Källquist, Julia Maibach, Maria Hahlin, Virginia Boix, Tamires Gallo, Foqia Rehman, Giulio D'Acunto, Joachim Schnadt, and Andrey Shavorskiy. HIPPIE: a new platform for ambient-pressure X-ray photoelectron spectroscopy at the MAX IV Laboratory. *J. Synchrotron Radiat.*, 28(2):624–636, Mar 2021.

[120] Štěpán Pick. On the electronic structure of surface Pt–Sn alloys. *Surface Science*, 436(1):220–226, 1999.

Scientific publications